UNIVERSITY OF NAPLES FEDERICO II

DOCTORATE IN
MOLECULAR MEDICINE AND MEDICAL BIOTECHNOLOGY

XXXIII CYCLE

Emanuela Senatore

"CENTROSOMAL TBC1D31 INTEGRATES cAMP SIGNALING AND OFD1 UBIQUITYLATION TO CONTROL CILIOGENESIS"

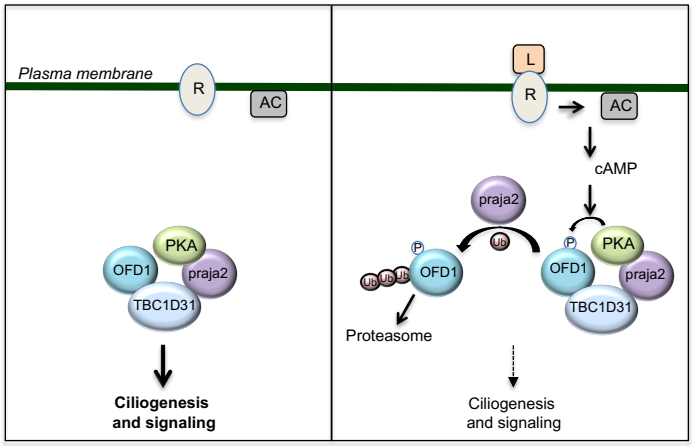

Year 2021

UNIVERSITY OF NAPLES FEDERICO II

DOCTORATE IN
MOLECULAR MEDICINE AND MEDICAL BIOTECHNOLOGY

XXXIII CYCLE

"CENTROSOMAL TBC1D31 INTEGRATES cAMP SIGNALING AND OFD1 UBIQUITYLATION TO CONTROL CILIOGENESIS"

Tutor
Prof. Antonio Feliciello

Candidate
Emanuela Senatore

Year 2021

Table of contents

List of abbreviations

α-tub	α-tubulin
AC	adenylate cyclase
Ac-tub	acetylated-tubulin
ADPKD	Autosomal dominant polycystic kidney disease
AKAP	A-kinase anchor protein
ARL13B	ADP-ribosylation factor-like protein 13B
BBS	Bardet-Biedel syndrome
cAMP	cyclic AMP
CBD	cyclic AMP binding domain
CHX	cycloheximide
CNG	cyclic nucleotide-gated ion channels
Co-Ip	Co-immunoprecipitation
DAV	distal appendage vesicles
DUB	deubiquitinating enzymes
EPAC	exchange protein activated by cAMP
FSK	Forskolin
γ-tub	γ-tubulin
GEF	Guanil exchange factor
Gli 1/2/3	Glioma associated oncogene
GPCR	G-protein coupled receptor
Gs	G stimulatory protein
HEK293	Human embryonic kidney cells
Hsp90	Heat shock protein 90
IFT	Intraflagellar transport
KD	Knock-down
LisH	Lis homology domain
NEK10	Nima-related kinase 10
NT	Non-transfected
OFDI	Orofacial digital type I

Ol	Oryzias latipes
PDE	phosphodiesterases
PKA	protein kinase A
PKAc	protein kinase A catalytic subunit
PKI	protein kinase inhibitor
Ptch1	Patched 1
RBR	ring between ring ligases
RI/RII	protein kinase A regulatory subunit I/II
SHH	Sonic Hedgehog
SMO	Smoothened
SUFU	suppressor of fused homolog
TZ	transition zone
Ub	ubiquitin
UPS	ubiquitin proteasome system

Abstract

The primary cilium is a microtubule-based organelle that regulates growth and development. Defects in ciliogenesis can lead to a group of genetic syndromes known as ciliopathies. The Oro-facial digital syndrome 1 (OFD1) is a X-linked ciliopathy caused by mutation in OFD1 gene, whose role in ciliogenesis is well established. Additionally, cAMP and ubiquitin pathway play a role in ciliogenesis. In mammals, most of the effects elicited by cAMP are mediated by protein kinase A (PKA). The cAMP-PKA pathway can induce activation of praja2, a RING E3-ubiquitin ligase of the ubiquitin-proteasome system (UPS). By a yeast two-hybrid screening, we identified TBC1D31 as a novel interactor of praja2. TBC1D31 is a protein localized at the centrosome and basal body, whose function is unknown. Given the role of centrosome in the control of primary cilia formation, the aim of my study was to investigate the role of TBC1D31 in ciliogenesis and evaluate the impact of cAMP and praja2 in TBC1D31-mediated ciliary functions.

We identified a scaffold complex assembled by TBC1D31 at centrosome that includes the ubiquitin ligase praja2, protein kinase A (PKA) and OFD1. We show that TBC1D31 is essential for ciliogenesis and for Medaka fish development. Upon cAMP stimulation, PKA phosphorylates OFD1 at ser735. Phosphorylation primes OFD1 to praja2-mediated ubiquitylation and proteasomal degradation. Removal of OFD1 promotes primary cilia resorption. Altogether, our findings indicate that TBC1D31 is a novel centrosomal scaffold protein that physically and functionally links the activation of the cAMP signalling to the regulation of primary cilium biology and development.

1. Introduction

1.1 cyclic AMP signaling pathway

Organisms need to respond to the physical and chemical changes in the environment around them; for this reason, most of multicellular organisms cells have the ability to emit and receive signals, such as hormones or growth factors. The reception of extracellular signals is allowed to the presence of a finely regulated signal transduction system, in which a receptor binds the signaling molecule and activates an intracellular signaling messenger, called second messenger. It, in turn, determines a biological response by acting on effector proteins, such as metabolic enzymes, proteins regulating gene transcription or proteins involved in cells proliferation and differentiation.

Cyclic AMP (cAMP) is the first second messenger to be identified and it is involved in a variety of biological functions (Sutherland 1958). cAMP levels are strictly and rapidly regulated by adenylyl cyclase (AC) and phosphodiesterases (PDEs). The AC is a transmembrane protein, with the catalytic site on the plasma membrane cytosolic side; in mammals, there are nine different AC regulated by G proteins and Ca2+ (Iyengar 1993). Upon an extracellular signal, AC rapidly generates cAMP from ATP, determining an increase of cAMP intracellular concentration. Conversely, PDEs reduces cAMP intracellular levels, by hydrolyzing cAMP in 5'-AMP (Francis 2011). PDEs are more then 50 and contribute to the specificity of cAMP signaling in time and also in its localization (Jin 1998).

The signaling molecules that lead to increased cAMP levels, act via G protein coupled receptors (GPCR). In human, there are more then 700 GPCRs, which constitute the largest family of membrane receptors. GPCRs are characterized by 7 transmembrane helix, with the N-terminal segment in the extracellular face and the C-terminal segment on the cytosolic side of the plasma membrane (Rosenbaum 2009). When activated by the binding of an extracellular molecule,

GPCRs undergo a conformational change that leads to the activation of G stimulatory proteins (G_s). G proteins are localized on the cytosolic side of the plasma membrane and are composed by three subunits: α, β and γ. When a GPCR is activated by the binding of a ligand, it acts as a guanyl exchange factor (GEF), exchanging GDP in GTP on the α subunit of the G_s protein. The presence of GTP makes the G_s protein active, causing the dissociation from β and γ subunits, and allowing the binding of $G_s\alpha$ protein to the target protein. In case of GPCR acting via cAMP, the Gα protein binds to and activates adenylate cyclase (Cooper 2014).

The Gα proteins are GTPases, indeed they inactivate themselves hydrolyzing GTP in GDP and stopping the signaling (Hepler 1992).
GPCRs have a fundamental role in living cells but, at the same time, their continuous stimulation can be deleterious. For this reason, when cells are exposed for a long time to a ligand, they carry out a process called receptor desensitization (Reiter 2006). This process starts with the phosphorylation of receptors, and then the binding of a class of proteins, called arrestin, that inhibit the interaction between receptors and G_s proteins; receptors are internalized and, in some cases, proteolyzed (Rajagopal 2018).
In mammals there are three effector proteins of cAMP: protein kinase A (PKA), exchange proteins activated by cAMP (EPACs), and cyclic nucleotide gated ion channels (CNGs) (Torres-Quesada 2017) (**Fig. 1**). Most of the cAMP effects depend on protein kinase A.

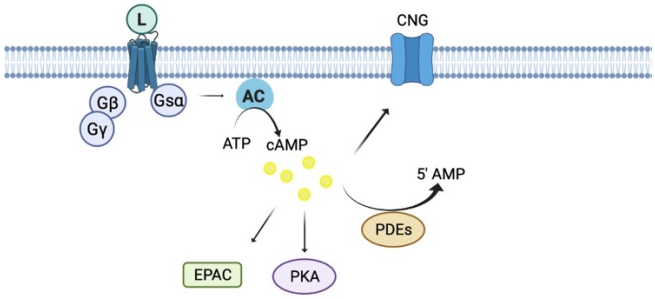

Figure 1. cAMP pathway. When an extracellular ligand binds a GPCR, the active trimeric G protein (Gsα) activates adenylyl cyclase (AC), that converts ATP in cAMP. The three principal effectors of cAMP in mammals are PKA, EPACs and CNGs. PDEs induces reduction of cAMP levels, by hydrolyzing it in 5'-AMP.

1.2 Protein kinase A

PKA was one of the first kinases to be isolated and cloned. It is a serine-threonine kinase, essential for the regulation of many cellular processes such as metabolism, gene transcription, cell growth and control of ion channels. PKA, in its inactive conformation, is a holoenzyme consisting of two regulatory (R) and two catalytic (C) subunits. In presence of cAMP, it binds to the R subunits causing the dissociation of the C subunits, which can thus phosphorylate the substrates (Taylor 1990) (**Fig. 2**).

The catalytic subunits are encoded by three different genes, α, β and γ (Taylor 1992) . The catalytic subunit consists of a smaller N-terminal lobe made up of beta strands with the ATP binding site, a linker and a larger C-terminal lobe that contains the catalytic portions and the substrates docking sites (Knighton 1991; Taylor 1993).

There are two different types of regulatory subunits, RI and RII, and two different isoforms of each type, α and β, so that in total there are 4 different regulatory isoforms, which differ in both localization and affinity for cAMP (Huang 1999). In fact, RI is mostly cytoplasmic and has a higher sensitivity to cAMP than RII which is mainly associated with specific cellular structures and organelles (Skalhegg 2000).

Despite these differences, the various isoforms have the same structural organization. At the N-terminus there is a dimerization/docking domain (D/D), which is necessary for binding of A-kinase anchor proteins (AKAPs) and for dimerization of the various subunits; in the middle, there is an autoinhibitory site and at the C-terminus, two cAMP binding domains (CBD), called A and B. CBD contains a phosphate-binding cassette, where the ribose phosphate of cAMP is anchored (Taylor 2005).

After the activation of AC, cAMP binds B site of R subunits, provoking a conformational change with the exposure of A site. When cAMP is bound to both CBD sites, Ser 39 in the autoinhibitory domain of R subunit is phosphorylated, leading to the dissociation of catalytic subunits (Taskén 2004;

Taylor 1990). The active catalytic subunits phosphorylate serine and threonine of substrate proteins, included in a specific consensus sequence (R-R-X-S/T).

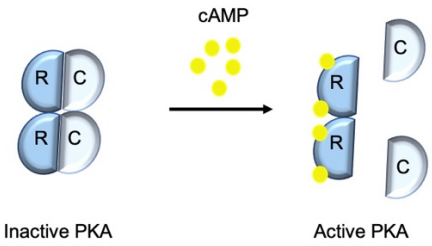

Figure 2. Activation of PKA. PKA, in its inactive form, is a holoenzyme constituted by two regulatory (R) and two catalytic (C) subunits. Two cAMP molecules bind each regulatory subunit, inducing a conformational change that led to the release of catalytic subunits. Dissociate catalytic subunits are active and can phosphorylate substrates.

The localization of PKA holoenzyme depends on AKAP proteins. AKAPs are proteins with similar features that targets PKA on specific substrates (Michel 2002). The first AKAP to be identified was the microtubule associated protein (MAP2) (Theurkauf 1982). AKAPs bind the D/D domain of R subunit through an amphipathic helix (PKA binding motif) of 14-18 conserved residues (Carr 1992; Newlon 2001). AKAPs have high affinity for the RII subunit (Carnegie 2003), but in some cases they bind also RI, with lower affinity (Burgers 2012; Burton 1997). The importance of AKAPs, is not only to target PKA near the substrates, but also, by binding the inactive holoenzyme, they make it subject only to the local cAMP and PDEs effect (Fraser 1999).

AKAP can also bind PDEs, thus providing an even major regulation of cAMP signaling in a specific site (Dodge 2001; Taskén 2001). Therefore, AKAPs constitute complexes, called transduceosome, in which are included not only PKA but also GPCR, AC and PDEs; these complexes allow to regulate the cAMP signaling locally, improving the response to extracellular signals (Feliciello 2001) (**Fig. 3**).

During cAMP stimulation, there is a phase in which cells begin to reduce their responsiveness to cAMP, called refractory phase; during it cAMP/PKA signaling is attenuated. This is due to reduction in C subunit transcription or

stability, activation of PDEs (often via phosphorylation by PKAc itself), proteolysis of various components of cAMP pathway, or binding of protein kinase inhibitors (PKI) to the C subunit (Armstrong 1995; Knighton 1991; Michel 2002; Rinaldi 2015). Moreover, it has been recently shown that signal attenuation depends also on the ubiquitylation and proteolysis of C subunit by the E3 ligase CHIP (Rinaldi 2019).

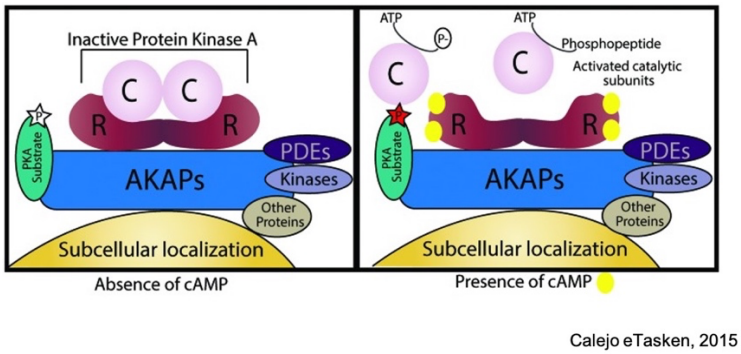

Figure 2. AKAP complexes. AKAPs target PKA in its inactive conformation near the substrates and in specific subcellular localization. AKAPs also bind PDEs, GPCRs and other signaling proteins generating complexes, called transduceosome, that regulate the cAMP signaling in a specific compartment.

1.3 The ubiquitin proteasome system

Proteolysis is a fundamental process for different biological function such as metabolism, growth and stress adaption. One of the proteostasis most important role is to avoid the formation of misfolded proteins during transduction, which would lead to the onset of diseases such as neurodegeneration and cancer (Dikic 2017).

Most of vertebrates cytosolic proteins are degraded via ubiquitin proteasome system (UPS), that is the first system for degradation of misfolded, damaged and short half-life proteins (Dikic 2017; Lilienbaum 2013).

UPS controls gene expression, metabolic pathways and activity or localization of signaling pathway molecules (Callis 2014).

UPS acts adding ubiquitin molecules to the substrates as a tag for degradation. Ubiquitin is a protein of 76 amminoacids, that binds to the lysine (K) of substrates (Husnjak 2012).

Substrates of the UPS can be modified in three different manner: monoubiquitylation, multi-mono ubiquitylation and polyubiquitylation. In monoubiquitylated proteins a single molecule of ubiquitin is added to lysin of substrates; in multi-mono ubiquitylated proteins, single molecules of ubiquitin are added on various lysins of the substrates; in polyubiquitylated proteins, polymers of ubiquitin are added on one or more lysin of the substrates (Callis, 2014). Ubiquitin has seven lysin and the ubiquitin chain can be assembled on each of them (Ikeda 2008). Each monomer of ubiquitin is bound with its C-terminal portion to the lysin of the substrate, or in case of polyubiquitin, to the lysin of the previous ubiquitin molecule.

Conjugation of ubiquitin to substates is performed through different reversible enzymatic reactions mediated by a complex of three proteins, E1, E2 and E3 (Husnjak 2012). E1 is the ubiquitin activation enzyme; in an ATP dependent reaction, ubiquitin is activated through the binding to a cysteine residue of E1, generating a thioester.

E2 is the ubiquitin conjugating enzyme; ubiquitin is transferred to it from E1, generating the E2-ubiquitin thioester. E2 enzymes are important in determining the type of assembled ubiquitin chain. E3 is the ubiquitin ligase; it binds substrates and lead to the formation of an isopeptide between the lysin of substrates and the C-terminal of ubiquitin molecules (Husnjak 2012).

Three different kinds of E3 ligases can catalyze the ubiquitin bond to substrates: HECT domain E3 ligases, RING domain E3 ligases and ring between ring (RBR) ligases. HECT E3 ligases are characterized by a cysteine residue that is the binding site for ubiquitin; ubiquitin is passed from E2 to HECT E3 and then to the substrate (Weissman 2001). RING E3 ligases bind E2 and substrates, allowing the ubiquitin passage directly from E2 to substrate (Metzger 2014). These enzymes have a RING domain constituted by 40-60 amminoacids with conserved residues of cysteine and histidine that bind two atoms of zinc (Zn).

More recently it has been identified a new kind of E3 ligase, RBR, characterized by the presence of two RING domains. RBR interacts with E2-ubiquitin complex and ubiquitin is passed to a cysteine residue of RBR and then to the substrate (Smit 2014).

In case of polyubiquitylation, three model of ubiquitin chain formation has been proposed. In the first model, ubiquitin molecules are added sequentially on the substrates; in the second model, the chain is assembled on E2 and then transferred to E3; the third model is a combination of the other two (Wiegering 2019) .

The position of ubiquitin, and the kind of ubiquitin-ubiquitin binding, determine the consequences of substrates ubiquitylation. Generally, ubiquitinations that involves lysin48 of ubiquitin, lead to degradation of substrates; instead, ubiquitinations involving lysin63 are related to non-proteolytic functions (Fu 1998; Haglund 2005). Moreover, monoubiquitylation is commonly associated with alteration of substrates localization or with alteration of protein complexes stoichiometry (Pohl 2019).

Ubiquitination is a reversible process. Deubiquitinating enzymes (DUBs) removes ubiquitin chains from substrates (Wilkinson 2009). There are more than 100 DUBs divided into five different families (Amerik 2004).

Proteins targeted for degradation by the UPS are proteolyzed into the proteasome 26S. The proteasome is a complex of several protein subunits and catalyzes the degradation of 80% of proteins in eukaryotic cells. It is constituted by proteins belonging to the AAA family, which induce conformational changes of the substrates, by hydrolyzing ATP (Bard 2018). The proteasome allows the digestion of polypeptides into small peptides of 2-10 residues (Kisselev 1999) (**Fig. 3**)

The proteasome consists of a central catalytic portion, 20S, and a regulatory portion, 19S, responsible for the recognition of substrates (Liu 2013). Two subunits are most important for substrates binding: Rpn10 (which has a ubiquitin-binding domain) and Rpn13 (Finley 2016); in some cases, the binding is indirect through other proteins that have ubiquitin-binding domains (Collins 2017). Once bonded to the substrate, the proteasome, via DUBs, disassembles and releases the ubiquitin molecules, which can be reused. Three main DUBs are associated with the proteasome: Rpn11, which is located at the entrance of the channel through which the substrate passes (Beck 2012), Usp14 (Borodovsky 2001) and Uch2 (Stone 2004).

Considering the importance of UPS system in different biological functions, an alteration of its activity is related to defects in the normal transduction of signaling pathways and related cellular processes (Wiegering 2019).

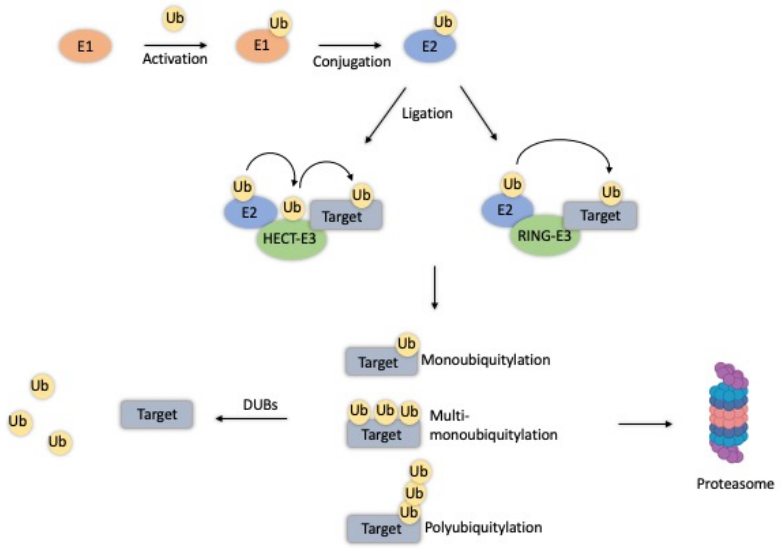

Figure 3. UPS system. Conjugation of ubiquitin to substrates occurs through three steps: binding of ubiquitin to E1 (activation), transferring of ubiquitin from E1 to E2 (conjugation) and association of ubiquitin to the substrates by E3 ligases. HECT-E3 ligases receive the ubiquitin from E2, and passes it to the substrates. RING-E3 ligases allow the passage of ubiquitin from E2 directly to the substrates. Substrates can be monoubiquitylated, multi-monoubiquitylated and polyubiquitylated. Ubiquitylated proteins are often degraded in the proteasome. Deubiquitinating enzymes (DUBs) removes ubiquitin from the substrates.

1.4 Praja 2

Praja2 is a protein belonging to the RING-H2 E3 ligase family. RING-H2 E3 ligases have as only difference from RING E3 ligases, the substitution of cystein4 with a histidine (Freemont 1993). The family of praja is constituted by two proteins, praja1 and praja2, that have a homology of 52.3%. Praja1 is a 78 kDa protein, encoded by a gene located on the X chromosome. Praja1 is highly expressed in different brain tissues and it has been associated with mental retardation (Yu 2002) . Furthermore, trough the regulation of tgf-β pathway, it has a role in tumorigenesis (Saha 2006).

Praja2 is encoded by a gene located on the long arm of chromosome 5, it is composed of 708 amino acids and has a molecular weight of 78 kDa. It is characterized by the presence of the RING-H2 domain in the C-terminal portion (amino acids 634-675).

Praja2 has a fundamental role in the cAMP pathway, in fact, it has an amphipathic helix constituted by aminoacids from 583 to 600, that is typical of AKAP proteins (Lignitto 2011). Thus, praja2 is an AKAP that binds RI and RII subunits of PKA and localizes the holoenzyme at plasma membrane, perinuclear region or in various cell organelles. During cAMP stimulation, praja2 ubiquitinates and degrades regulatory subunit of PKA, supporting cAMP signaling. Therefore, it plays a fundamental role in generating and sustaining a localized activation of PKA (Lignitto 2011).

Several roles have recently been attributed to this E3 ligase in different cellular processes, in many cases related to cAMP pathway.

For example, through regulation of Mob1, praja2 has an important role in proliferation of glioblastoma. Mob1 is a positive regulator of the tumor suppressor Hippo cascade and it has been identified as a substrate of praja2. In proliferating cells, praja2 ubiquitinates and degrades Mob1, causing attenuation of the Hippo pathway and supporting the growth of glioblastoma (Lignitto 2013).

Another important role of praja2 related to growth of cancer cells depends on the regulation of MAPK cascade mediated by praja2. Praja2 ubiquitinates and induces proteolysis of kinase suppressor of ras (Ksr1). Ksr1 is a component of a complex that promotes raf family member phosphorylation and contributes to the activation of ERK. Praja2, inducing Ksr1 proteolysis, is involved in regulation of cancer cells growth and in maintenance of undifferentiated pluripotent state of mouse embryonic stem cells (Rinaldi 2016). This mechanism has been recently confirmed also in gastric cancer cells (Zhao 2021).

Furthermore, praja2 has also a role in cAMP-mediated neuronal differentiation and growth. It ubiquitinates and promotes degradation of NOGO-A, an inhibitor of neuronal growth in the mammalian brain (Sepe 2014).

Moreover, it also plays a role in glucose homeostasis and stem cell differentiation. Praja2 ubiquitinates and degrades TCF/LEF1, that are transcription factors of Wnt/β-catenin pathway. Through this mechanism, praja2 inhibits Wnt/β-catenin pathway and regulates stem cells differentiation (Song 2018).

Finally, praja2 is also involved in macrophage polarization. It ubiquitinates MFHAS1, a potential oncogene, positively regulating Jnk/p38 pathway and inducing macrophage polarization (Zhong 2017).

Figure 4. Praja2 substrates. Praja2 ubiquitinates several target proteins involved in different cellular processes.

1.5 The primary cilium

Cilia are microtubule-based organelles highly conserved throughout eukaryotic evolution, that protrude from the cells surface. These complex structures are divided into two subtypes: motile and non-motile. Motile cilia protrude in large number from a single specialized cell, such as cells of respiratory epithelium. They are involved in mucus clearance, cerebrospinal fluid flow and ovum transport (Spassky 2017).

Non-motile cilia (primary cilia) are present in a single copy in almost all type of human cells (Mitchison 2017). Primary cilia act as antennae that receive signals from the extracellular space and convert them into signaling cascades that start within the ciliary compartment, and then are transduced to the cell body. Several important functions of primary cilia have recently been identified such as growth, development, differentiation and metabolism (Satir 2010).

Cilia consist of a basal body, a transition zone (TZ) and of an axoneme that is surrounded by the ciliary membrane, continuous with the plasma membrane. The axoneme is constructed from nine doublets of microtubule, known as outer doublets, surrounding a central pair in the motile cilia (the 9 + 2 arrangement); this central pair is loss in primary cilia (the 9 + 0 arrangement) causing their immobility (Satir 2007). The axoneme structure is subjected to different post-translational modification such as acetylation, glutamylation and glycylation that contributes to the assembly and stability of primary cilia (Ishikawa 2011). The basal body derives from the mother centriole and anchors the axoneme at the cell body surface. The TZ localizes between the basal body and the axoneme and it is important for the compartmentalization of cilium, because it forms a gate that controls the entry and exit of proteins in the ciliary compartment (Avidor-Reiss 2015).

Primary cilia emerge from centrosome through a mechanism by which one centriole of the centrosome transforms into the basal body (**Fig. 5**).

During G0 or G1 phase of cell cycle, the centrosome is constituted by a pair of centrioles (mother and daughter) surrounded by a membranous material, known as pericentriolar matrix. During the S phase, occurs the duplication of the centriole, and at the proximal end of both centrioles, starts to grow a new single one. The mother and daughter centriole have some differences, in fact the mother centriole has two sets of projection at the distal end, called distal and subdistal appendages, that are required for primary ciliogenesis (Piel 2000). The centrioles are formed by nine triplets of microtubules arranged around a central axis; each triplet contains one complete (A tubule) and two incomplete (B tubule and C tubule) tubules (Winey 2014). When cells exit the mitotic cycle in response to nutrient deprivation or other causes, different events cause the remodeling of the distal end of the mother centriole transforming it into the basal body. In this condition, small cytoplasmic vesicles generated from the Golgi and from the recycling endosome, called distal appendage vesicles (DAVs), start to accumulate near the distal appendages of the mother centriole (Schmidt 2012). The vesicular fusion generates a membranous cap, named first ciliary vesicle, on the distal tip of the mother centriole, that is the first sign of the centriole to basal body transition (Sorokin 1968). Below this cap, microtubules start to elongate, transforming the triplets of the basal body into doublets typical of the axoneme structure (the C-tubule of centrosome terminates within the TZ, instead A and B tubule continue to extend). At the same time, the vesicular trafficking enlarges the cap, enclosing the growing axoneme in a double membrane. This growing cilium migrates and sticks under the plasma membrane; the fusion of the plasma membrane with the ciliary one creates continuity of two these compartments (Sánchez 2016).

The axoneme microtubules undergo a series of post-translational modifications such as acetylation, detyrosination, polyglutamylation and polyglycylation. Acetylation on lysine 40 is the main post-translational modification that occurs on the luminal surface of α tubulin and stabilizes the axoneme (Cueva 2012; L'Hernault 1983).

Since ribosomes are absent in cilia, the extension of the axoneme and its maintenance require the import of proteins from cytoplasm. Microtubules in the axoneme elongate incorporating tubulin subunits at the axoneme tip (Johnson 1992). The intraflagellar transport (IFT) is the principal pathway that allows to incorporate and move protein into the cilia (Kozminski 1993). IFT trains are polymers of IFT proteins which, interacting with motor proteins, traffic cargoes up and down the cilium (Wingfield 2017). This system is responsible not only of the movement of protein from the basal body to the tip (anterograde transport), but also for the return of protein from the tip to the basal body (retrograde transport). Kinesin 2 is the principal motor protein involved in the anterograde transport; dynein is responsible of the retrograde transport (Cole et al., 1998; Signor et al., 1999). The IFT particles are subdivided in IFT-A and IFT-B complexes. The IFT-B subcomplex is constituted by sixteen polypeptides involved in the anterograde transport; the IFT-A subcomplex is composed by six polypeptides involved in the retrograde transport and also in the returning of IFT-B proteins to the base of cilia (Pazour 1998). Transport mediated by IFT proteins consists of four phases: complex assembly at the basal body, passage through the TZ, transport of cargoes to the ciliary tip by the anterograde movement and transport of the cargoes to the ciliary base by retrograde transport (Webb 2020). This last step is due to the remodeling of anterograde trains into retrograde trains, supported by modification in kinesin 2 at the cilia tip (Craige 2014).

Another important complex that moves in association with IFT is the BBSome, composed by eight BBS proteins. BBSome plays a fundamental role in regulation of IFT assembly and turnaround in cilia; actually, it is involved in the assembly of IFT at the ciliary base and it binds the anterograde IFT particles, reaching the ciliary tip to regulate IFT recycling (Wei 2012).

Cilia disassembly is also an important process, strictly dependent on the cell cycle phase, but the mechanism by which this process occurs are not completely understood. There are a lot of proteins that regulate this process, including the scaffolding protein HEF1 and the calcium-calmodulin activate Aurora A kinase, that, respectively, induce enter in mitosis and deacetylation of axoneme tubulin (Plotnikova 2012; Pugacheva 2007).

Cilium disassembly requires also destabilization and depolymerization of microtubules; the protein family of kinesin-13 is involved in this process. In particular, Kif2a, is activated by phosphorylation during growth signals stimulation and exhibits microtubule-depolymerizing activity at the mother centriole, leading to disassembly of primary cilium. Cells deficient of Kif2a, are not able to disassembly cilia after growth stimulation (Miyamoto 2015).

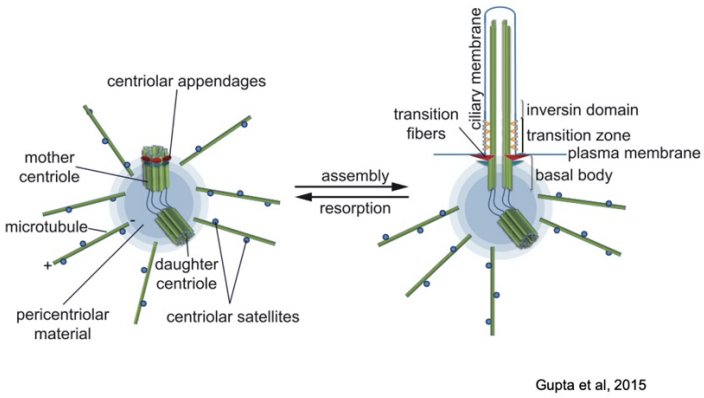

Figure 5. Primary cilia structure. Primary cilia consist of a basal body and an axoneme, surrounded by the ciliary membrane, continuous with the plasma membrane. The basal body derives from the mother centriole of the centrosome. Axoneme and basal body are separated by the transition zone, that regulates passage of proteins in and out ciliary compartment.

The presence of primary cilium is closely related to the phase of cell cycle; cells in G0 phase are highly ciliated, cells in G1, S and G2 are poorly ciliated and cells in M are non-ciliated (Plotnikova 2009). To allow this, the assembly and disassembly of cilia are highly dynamic and must be finely tuned. Both the

ubiquitin-proteasome system and autophagy, which represent the main protein degradation systems within the cell, are involved in this dynamic regulation of primary cilia structure and function.

The UPS system is involved in degradation of protein necessary both for the assembly and for the disassembly of cilia. Proteomic analysis revealed the presence of several E1 and E3 ligases and also DUB at the base or along the primary cilia (Mick 2015); although most of substrates of these enzymes have not been identified, their localization in the cilia suggests the importance of the ubiquitin-proteasome system in this organelle. Some examples of ubiquitinated ciliary proteins have been described. CP110, that is a negative regulator of primary ciliogenesis localized at the centrosome, is regulated by two E3 ligases (SCF and EDD-DDB1) that ubiquitinate it inducing cilia formation and also by a DUB (USP3) that deubiquitinates it (D'Angiolella et al., 2010; Li et al., 2013). UPS controls ciliogenesis also during axoneme elongation: the E3 ligase CRL3 ubiquitinates and remove trichoplein, that binds Aurora A kinase at the centrosome. The degradation of trichoplein leads to inactivation of Aurora A kinase and induction of primary ciliogenesis (Kasahara 2014). Similarly, the disassembly of primary cilia is regulated by UPS. Thus, the E3 ligase APC ubiquitinates Kif2a in quiescent cells abrogating its capacity to induce cilia disassembly. NEK10, a kinase essential for cilia formation, is ubiquitinated and degraded by the E3 ligase CHIP, inducing cilia resorption (Porpora 2018).

As well as the ubiquitin proteasome system, autophagy is involved in the regulation of ciliogenesis. At least 12 ATG proteins have been identified that localize along the ciliary axoneme and a large number also in the basal body, indicating the involvement of autophagy in ciliary formation or function (Pampliega 2013). However, the role of autophagy in ciliogenesis is still debated. MEF knocked down for ATG5 formed longer cilia then wild type cells, indicating that autophagy reduces cilia growth. In addition, autophagy in basal condition limits the enter of IFT20 in the cilium, causing a reduction in the traffic of component required for cilia growth (Pampliega 2013). At the same time, it

has also been demonstrated that autophagy induced by starvation leads to the formation of primary cilia by removing OFD1, a protein located at the centrosome and at the pericentriolar matrix (Tang et al., 2013).

The principal role of primary cilia is to transfer extracellular signals to the cell body. Actually, primary cilia are enriched of receptors, in particular GPCRs, and signaling molecules; each point of cilia structure is crucial to support this signaling pathways (Mykytyn 2017). Sonic Hedgehog (SHH) is the most important pathway identified within the primary cilium. It is involved in development and stem cells maintenance. Most of components of the pathway are located within the cilia (Goetz 2010).

Patched 1, in absence of ligand, inhibits the activity and the accumulation of smoothened (SMO), a seven transmembrane protein (Rohatgi 2007). In this condition, SUFU interacts with gli proteins that are proteolyzed and act as transcriptional repressors (in particular Gli3). The binding of hedgehog ligand to Patched 1, leads to the activation of SMO, which translocates into the cilium. Here, SMO inhibits the interaction between SUFU and gli proteins, that in non-proteolyzed form function as transcriptional activators of gene involved in proliferation, differentiation, survival and growth (in particular gli2) (Robbins 2012; Ruiz i Altaba 2002) (**Fig. 6**).

Considering that most of SHH pathway proteins are located within the cilia, both IFT and basal body proteins are required for response to this pathway (Bangs 2017; Huangfu 2003).

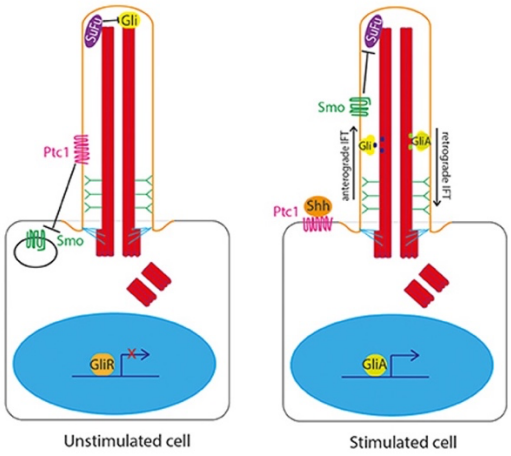

Wheway et al, 2018

Figure 6. Sonic Hedgehog pathway. In unstimulated cells, the GPCR Ptc1, inhibits the activity of SMO and SUFU interacts with gli proteins, leading to their processing. In proteolyzed form, gli functions as a transcriptional repressor. When Shh ligand interacts with Ptc1, SMO is active and inhibits the interaction between SUFU and gli. Gli proteins, in their non-proteolyzed form, act as transcriptional activator of genes involved in development, survival and growth.

Alterations in function or structure of primary cilia can lead to a broad spectrum of genetic disorders, known as ciliopathies (Badano 2006). The hypothesis that alteration in primary cilia could be related to human disorders came out when it was discovered that polycystin 1 gene, responsible of polycystic kidney syndrome, was located within the cilium (Barr 1999).

Ciliopathies could be due to alterations in cilia assembly, maintenance and disassembly, or to alterations in trafficking and signaling pathways within the cilia. The most common phenotypic manifestations of ciliopathies include kidney diseases, retinal degeneration, obesity, hepatic cysts, polydactyly, mental retardation and skeletal defects (Davis 2012). The number of ciliopathies reported is 35, but it is constantly growing, as well as the number of genes associated with ciliopathies. In addition, a very large number of candidate genes

that could be associated with ciliopathies have been identified, but they have yet to be verified (Reiter 2017).

Polycystic kidney syndrome (ADPKD) was the first ciliopathies identified; it is caused by mutation in polycystin 1(PKD1) and polycystin 2 (PKD2) genes, which are essential for renal tubules differentiation and act as mechanosensors at the ciliary compartment (Torres 2007).

Most of ciliopathies are caused by alterations in the assembly of primary cilia structures. Mutations in centrosomal or basal body proteins are responsible for several ciliopathies such as Joubert's syndrome, orofacial-digital type 1 (OFDI) syndrome, nephronoptisis and Bardet-Biedel syndrome (BBS). Joubert's syndrome is caused by mutations in the centrosomal protein CEP290 or even by mutation in Talpid 3, a protein of the distal appendages of the centrioles (Alby 2015; Parisi 2004).

OFDI syndrome is caused by mutations of OFD1, a protein located at centrosome and pericentriolar matrix (Romio 2003).

Bardet-Biedel syndrome is one of the best-known ciliopathies. It is associated with mutations of BBSome, that alter the transport of protein within the cilia causing defects in ciliary functions and leading to manifestations of several symptoms (Blacque 2006).

Developmental alterations represent the most common phenotypic manifestation of ciliopathies. These alterations are mostly related to disruption of SHH pathway, whose loss of activity causes birth defects (McMahon 2003).

1.6 cAMP and cilium

The primary cilium, functioning as an antenna that receive extracellular signals and transmits them into the cell body, is enriched of receptors (in particular GPCRs) and signaling molecules. GPCRs have a consensus sequence, called ciliary localization sequence, that allow their transport from the Golgi to the primary cilium (Berbari 2008).

The amount of receptors and signaling molecules within the cilia is different from that of the cell body, thus generating an environment rich in signal pathways (Hilgendorf 2016).

cAMP is one of the majors signaling molecules located within the cilia. The earliest examples of cAMP role in cilia was discovered in the olfactory neurons. In these cells, odors lead to the activation of GPCRs that stimulate cAMP production by AC3; cAMP activates the cyclic nucleotide-gated ion channels, leading to depolarization that is transmitted from the cilia to the synapses (Kaupp 2010).

In the cilium there are high levels of cAMP, five times more than the whole cell; this depends mainly on the activity AC5 and AC6 (Moore 2016). The main effector of cAMP within the ciliary compartment is protein kinase A. Both catalytic and regulatory subunits of PKA are located in the cilia. They were initially identified in the basal body region, but it was later proved their localization in the ciliary shape (Barzi 2010; Mick 2015; Tuson 2011). The anchoring of PKA at the cilium is controlled by AKAP (Barzi 2010; McConnachie 2006).

The main role so far identified of cAMP and PKA in the cilium is the regulation of the Sonic Hedgehog pathway. PKA negatively regulates Shh pathway by phosphorylating and inducing proteolysis ofgli2and Gli3, thus activating their function of transcriptional repressor (Tempé 2006). In addition, PKA phosphorylates SUFU, stabilizing it in complex withgli2and Gli3 and favoring their proteolysis even more (Chen 2011).

At the same time, the Shh pathway negatively regulates the activity of PKA. Indeed, the seven transmembrane protein SMO, acting through an inhibitory Gα protein, reduces cAMP levels in response to Sonic Hedgehog (Ogden 2008). Moreover, Gpr175 receptor, upon Shh pathway activation, localizes within the cilium, couples with inhibitory Gα proteins and inhibits cAMP production (Singh 2015). It was later shown that Shh reduces cAMP levels mainly through entry of calcium, rather than through the activation of inhibitory Gα protein (Moore 2016).

Gpr161 is an orphan GPCR that has a fundamental role in localization of PKA within the cilium and in antagonization of the Shh pathway; in fact, its loss leads to hyperactivation of Shh pathway (Mukhopadhyay 2013). Gpr161 acts as a high affinity AKAP for RI subunits of PKA. It increases cAMP levels, coupling with a Gα stimulatory protein. Gpr161 is a substrate of PKA, thus mutations in the kinase phosphorylation sites alter the ciliary localization of the receptor (Bachmann 2016).

When Shh is activated, Gpr161 is released from cilia and cAMP levels are reduced (Mukhopadhyay 2013) (**Fig. 7**).

ARHGAP36, a rho GTPase activating protein, represents another connection between PKA and Shh pathway. It reduces the sensitivity of cells to cAMP, inducing intraciliary ubiquitylation and lysosomal degradation of PKA catalytic subunit. The inhibition of PKA by ARHGAP36 promotes Shh pathway (Eccles 2016).

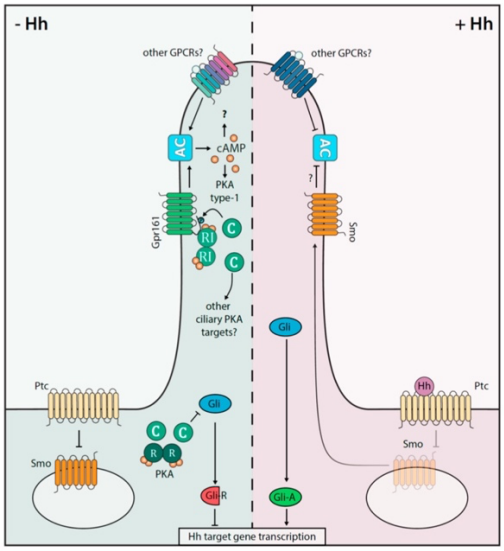

Tschaikner et al, 2019

Figure 7. cAMP and Shh pathway. In absence of Shh ligand, Gpr161 increases cAMP levels in the cilium and contributes to the activation of PKA. PKA phosphorylates gli proteins, inducing their proteolysis and thus inhibiting Shh pathway. In presence of Shh ligand, Gpr161 is released from the cilium and cAMP ciliary pathway is inhibited.

PKA is also involved in the control of cilium length. In part, this regulation depends on the phosphorylation of NEK10 by PKA. NEK10 is a kinase essential for the formation of primary cilia; in serum deprived cells, PKA phosphorylation induces NEK10 ubiquitylation and proteolysis mediated by the E3 ligase CHIP, resulting in cilium disassembly. This therefore demonstrates that PKA plays a key role in inducing cilia resorption (Porpora 2018) (**Fig. 8**).

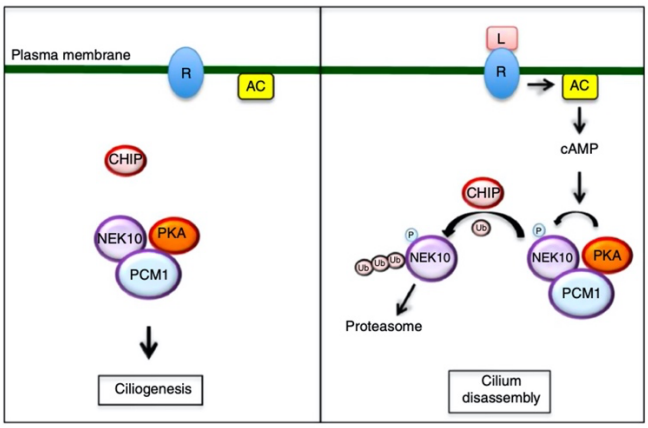

Porpora et al, 2018

Figure 8. cAMP induces primary cilium disassembly. In growth arrested condition, NEK10 promotes the formation of primary cilium. Production of cAMP induces NEK10 phosphorylation mediated by PKA. Phosphorylated NEK10, is ubiquitinated by E3 ligase CHIP and proteolyzed. The proteolysis leads to cilium disassembly.

Conversely, cAMP promotes ciliogenesis in serum supplemented confluent cells. In epithelial and mesenchymal cells, the raise of cAMP levels, increases cilium length by enhancing the velocity of anterograde flux, but not the one of the retrograde (Besschetnova 2010).

Through an approach based on the use of nanoparticles, it has been shown that the compartmentalization of cAMP plays a fundamental role in determining its effect on ciliary dynamics. In fact, the amount of cAMP located inside the cilium, determines an increase in its length; conversely, cytoplasmic cAMP leads to cilia length reduction (Hansen 2020).

In addition to PKA, also phosphodiesterases (PDEs) are localized and play a role within the cilia. PDE1c has been identified in the olfactory neuron's cilia (Cygnar 2009); PDE6d localizes in the cilium and it is involved in the entry of preylated proteins (Humbert 2012).

1.7 OFD1

OFD1 is a protein localized at the centrosome and basal body, whose mutation are responsible of a genetic syndrome known as Orofacial digital type 1 syndrome.

The orofacial digital syndromes (OFD) are a group of developmental genetic disorders, identified among ciliopathies. There are nine different forms of OFD, that share phenotypical features, especially malformation of face, oral cavity and digits (Macca 2009). The orofacial digital type 1 syndrome was described for the first time by Psaume in 1954. It is the most common type of OFD with an incidence of 1:50000 live births, and no differences determined by the race (Wahrman 1966). It is easily distinguishable from the other OFD thanks to a typical X-linked transmission, with male mortality during first and second pregnancy trimester; anyway, some cases of affected male were reported (Macca 2009).

The phenotypic anomalies are in common with the other types of orofacial digital syndromes and also with other kinds of ciliopathies. The principal phenotypic features are malformations of the face (cleft in the upper lip, frontal bossing, prominent root of the nose, facial asymmetry, variable degree of alopecia), oral cavity (multilobulated tongue, cleft or high arched palate, supernumerary teeth) and digits (rachydactyly, syndactyly, polydactyly), defects in the brain structure, developmental defects, kidney cysts and in some cases mental delay (Macca 2009).

The gene responsible for this syndrome is OFD1 gene, located on the Xp22.2-Xp22.3 region (Feather 1997; Ferrante 2001). This gene generates a protein of 1012 aminoacids that has a Lis homology (LisH) domain at the N-terminal portion and downstream of it, five coiled-coil domains (de Conciliis 1998). The LisH domain is involved in cell migration, nucleokinesis and chromosomal segregation (Emes 2001).

OFD1 is localized at the centrosome (Romio 2003), and also at the base of the primary cilium in post mitotic cells (Giorgio 2007; Romio 2004). More

specifically, it has been demonstrated that OFD1 localizes at the distal end of both centrioles (mother and daughter) and it is strictly associated with microtubules; in fact, it is in complex with α and γ tubulin (Singla 2010). A quote of OFD1 also localizes in the nucleus, where it interacts with RuvBl1, a protein of the AAA+ family of ATPases, involved in the control of cell division and transcriptional regulation and associated with the formation of kidney cysts (Giorgio 2007).

Finally, OFD1 is an important component of centriolar satellites, as well as BBS4 and Cep290. The N-terminal portion of OFD1 is necessary for its localization at the centriolar satellites. In this compartment, OFD1 binds BBS4 and this functional interaction determines morphogenesis (Lopes 2011).

OFD1 has an important role in the regulation of centriole length and distal appendages. It acts as a cap that stabilizes centriolar microtubules at a specific length; actually, cells with mutation in OFD1 gene show instability of centriolar microtubules and also alteration of centriolar length. Moreover, OFD1 absence affects also the structure of distal appendages, that are required for the formation of primary cilia (Singla 2010).

The principal role of OFD1 is its involvement in primary ciliogenesis; in fact, cells lacking OFD1 are unable to form primary cilia (Corbit 2008).

The use of animal models provided a lot of information about OFD1 function both in physiological and pathological conditions. Murine models of heterozygous female with deletion of exons 4 and 5 of OFD1, generate a truncated mRNA of 106 aminoacids; whereas male embryos die. The female mice have a phenotype similar to the one generated by the human disease. This phenotype is mostly related to cilia alteration. In fact, primary cilia are absent in the 50% of kidney cysts cells, instead, they are present in the non- cystic glomerulus and in the normal kidney tubules (Ferrante 2006). OFD1 is essential for the formation of the ciliary axoneme; thus, in heterozygous female mice limb cells the ciliary axoneme is shorter and malformed, instead the basal body is normal (D'Angelo 2012).

OFD1 is also important for the left-right asymmetry; the expression of gene such as Nodal (that is expressed only in the left lateral plate mesoderm) is bilateral in the male mice embryos, who die, instead, it is normal in the female mice and in wild type mice (Ferrante 2006). These anomalies probably depend on altered capacity of ciliogenesis, in fact, they were described also in other mice with mutations of genes involved in primary cilia formation (Pennekamp 2002). The heterozygous mice have also defects in brain development, with a variable phenotype from middle to severe (D'Angelo 2012), due to the X-inactivation that occurs in mice, but not in human (de Conciliis 1998). Expression of Shh pathway components is altered in the neural tube, in fact Ptch1 andgli1are reduced in the male neural tube, and to a minor extent, also in female mice (Ferrante 2006). Conversely, in the brain there is a higher activation of Shh pathway, due to increased expression ofgli2and Ptch1 in the dorsal telencephalon (D'Angelo 2012).

Analysis in Zebrafish, that expresses a homologous of the human OFD1 with a 29,6 % of identity, show that OFD1 always localizes at centrosome/basal body and also in the nucleus. Zebrafish silenced for OFD1 show a typical ciliary phenotype, with curved body, laterality defects, hydrocephalus and edema. Also in this case, the phenotype is related to alteration in primary cilia, thus in mutant Zebrafish cilia are shorter, confirming that OFD1 is necessary for axoneme formation and maintenance. Therefore, the phenotype observed in Zebrafish is comparable to that of mouse models and confirms the importance of OFD1 in the formation of primary cilia and in brain development, and also its involvement in the pathogenesis of kidney cysts (Ferrante 2009).

At molecular level, the role of OFD1 in ciliogenesis, among others, is related to its capacity to recruit IFT88, an important protein of the IFT-B complex. Actually, in cells without OFD1, IFT88 is not associated at the centrosome, allowing ciliogenesis inhibition (Singla 2010).

The distal appendages of centrioles play a crucial role in primary cilia formation, so the ability of OFD1 to regulate their structure is another way through which it is involved in ciliogenesis (Singla 2010).

The population of OFD1 localized at the centriolar satellites has a different role in primary ciliogenesis. Thus, pericentriolar OFD1 has an important role in inhibiting ciliogenesis, unlike the centriolar one. It binds BBS4, preventing its translocation inside cilia and blocking ciliogenesis. During serum starvation, pericentriolar portion of OFD1 is removed by autophagy, allowing the release of BBS4 with consequent correct formation of primary cilium (Tang 2013)(**Fig. 9**).

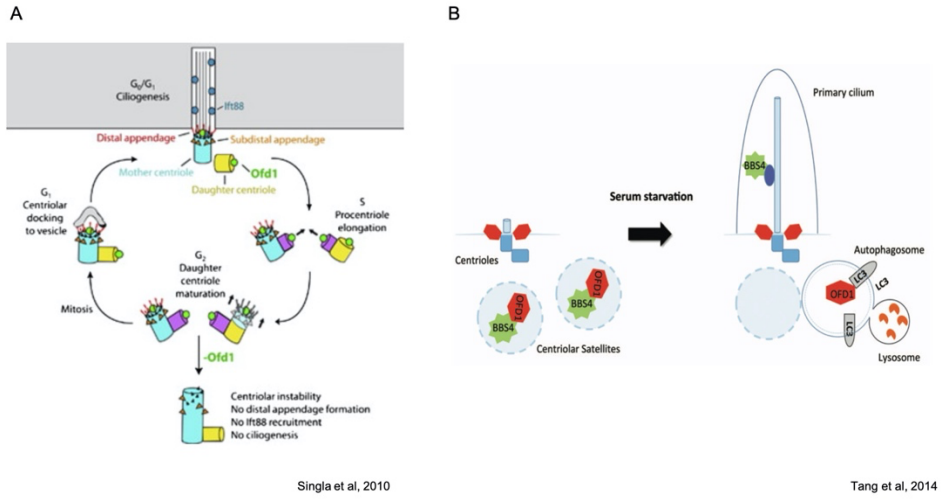

Figure 9. Dual role of OFD1 in primary ciliogenesis. (A) Centrosomal OFD1 is involved in the maturation of centriole during G2 phase of the cell cycle. It also recruits Ift88 at the mother centriole, allowing cilia formation in G0/G1 phase. (B) Pericentriolar OFD1 inhibits primary ciliogenesis, retaining BBS4. In serum deprivation, pericentriolar OFD1 is removed by autophagy, leading to BBS4 translocation and cilia formation.

Mutations of OFD1 are observed in the 80% of patients with orofacial digital syndrome (Thauvin-Robinet 2009). More than 130 OFD1 mutations have been identified; they occur throughout the gene, without hotspot region (Franco and Thauvin-Robinet 2016; Romio 2003). There is a lot of variability in the type of

mutations identified and often without correlation between the type of mutation and the phenotype (Prattichizzo 2008). About the 30% of mutation are point mutation (including missense, non-sense and splice site), 58% are frameshift and about 20% are deletions that cause premature stop codon (Macca 2009; Prattichizzo 2008).

The analysis of mutations in the different regions of the gene, demonstrate that LisH domain is fundamental for all OFD1 function including recruitment of Ift88 and Cep164, whereas mutations downstream the LisH domain are most important for the regulation of centriolar length. Thus, mutations in LisH domain completely block ciliogenesis, instead mutations in the C-terminal domain cause only a reduction of primary cilia formation (Singla et al., 2010).

2. Aim of the study

The primary cilium is a microtubule-based organelle involved in key biological function. Formation of primary cilium is a finely regulated process that starts with the rearrangement of the centrosome into the basal body. Defects in primary ciliogenesis can lead to a group of genetic disorders, known as ciliopathies. Among them, the orofacial digital syndrome type I is caused by mutation in OFD1 gene.

Recently it has been identified an important role of cAMP/PKA and UPS system in promoting disassembly of primary cilia (Porpora 2018), but their role in ciliogenesis is still debated.

Praja2 is a RING-H2 E3 ubiquitin ligases, mostly regulated by cAMP, that is carefully studied in the laboratory where I performed my PhD program.

We identified TBC1D31, a centrosomal protein with unknown function, as a novel interactor of praja2, by a yeast two hybrid screening. Moreover, it has been previously demonstrated that centrosomal protein OFD1 takes part to the interaction network of PKA (Rinaldi 2019), and also it has been identified as an interactor of TBC1D31, by the use of bioinformatic tools.

Given the role of centrosome/basal body in control primary cilium formation, the aims of my study were to:

- characterize the complex assembled by TBC1D31/praja2/OFD1/PKA at the centrosome;
-investigate the role of TBC1D31 complex in primary ciliogenesis
-investigate the regulation of TBC1D31 complex by the GPCR-cAMP pathway and its impact in primary ciliogenesis.

3. Materials and methods

Cell lines and tissues. Human embryonic kidney cell line (HEK293) and NIH3T3 were cultured in Dulbecco modified Eagle's medium containing 10% fetal bovine serum in an atmosphere of 5% CO_2.

Plasmids and transfection. Vector encoding for GFP-TBC1D31 were provided by Dr Raught B. and Dr Pellettier R.; flag-OFD1 and myc-OFD1 were provided by Dr Franco B.; vectors encoding praja2 and ubiquitin were previously described (Sepe 2014) (Carlucci, 2008); praja2 inactive mutant (praja2rm) carrying cys634 and cys637 changed to alanine was used; flag-E97G and praja2 Δ550-570 was purchased from Genscript; pEF5B-FRT-cilia-APEX (APEX-GFP) was purchased from Addgene; TBC1D31 mutant (940-970) and OFD1 mutants were generated by PCR using specific oligonucleotides. siRNAs targeting praja2 and TBC1D31 were purchased from Dharmacon and Life technologies respectively. siRNAs were transfected using Lipofectamine 2000 (Invitrogen) at a final concentration of 100 pmol/ml of culture medium.

The siRNA sequences of TBC1D31 (Life Technologies) are:

sequence 1: 5'- GGAAUGCACUUACAAGAUTT- 3'

sequence 2: 5'- GCUACUCAGAGUAUUACAGTT- 3'

The siRNA sequences of Praja2 (Dharmacon) are:

sequence 1: 5'- GAGAUGAGUUUGAAGAGUU- 3'

sequence 2: 5'- GGGAGAAAUUCCUUGGUUA- 3'

sequence 3: 5'- UGACAAAGAUGAAGAUAGU- 3'

sequence 4: 5'- UCAGAUGACCUCUUAAUAA- 3'

Antibodies and chemicals. The following primary antibodies were used: mouse GFP (1:1000 immunoblot; 1:50 immunoprecipitation; catalog # 11814460001 Roche), mouse flag (1:3000 immunoblot, 1:200 immunoprecipitation; 1:1000 immunofluorescence; F3165 Sigma), mouse GST (1:5000; catalog # sc-138 Santa Cruz), rabbit praja2 (1:1000 immunoblot, 1:200 immunofluorescence; catalog # A302-991A Bethyl), mouse γ tubulin (1:300; catalog # sc-17788 Santa Cruz), rabbit TBC1D31

(1:100 immunofluorescence; catalog # ab121771 Abcam), rabbit TBC1D31 (1:1000 immunoblot, 1:100 immunoprecipitation, 1:100 immunofluorescence; Primm), mouse HA.11 epitope (1:1000; catalog # 16B12 BioLegend), rabbit OFD1 (1:1000 immunoblot; catalog # ABC961 Millipore), rabbit OFD1 (1:100 immunofluorescence; catalog # HPA031103 Sigma), rabbit Phospho-(Ser/Thr) PKA Substrate (1:1000; catalog # 9621S Cell Signaling), mouse acethylated tubulin (1:400; catalog # T7451 Sigma), rabbit acetylated tubulin (1:400; catalog # ab125356 Abcam), mouse myc (1:1000 immunoblot, 1:200 immunoprecipitation; catalog # M4439 Sigma), mouse tubulin (1:5000; catalog # T6199 Sigma), mouse Hsp90 (1:5000; catalog # 60318-1-Ig Cell Signaling), rabbit Hsp70 (1:5000; catalog # 10995-1-AP Cell signalling), mouse PKAc (1:1000; catalog # sc-28315 Santa Cruz). Antibody protein complexes were detected by HRP-conjugated antibodies (Biorad) and ECL (Euroclone).

The following chemicals were used: Forskolin (40 μM; catalog # F3917 Sigma), H89 (10 μM; catolog # 19-141 Sigma), Chycloheximide (100 μM; catalog # 01810 Sigma), MG132 (10 μM; catalog # C2211 Sigma), Puromorphamine (1 μM; catalog # ab120933 abcam).

Immunoprecipitation, pull down assays and immunoblot. Cells were lysed with buffer 0.5% NP40 (150 mM NaCl, 50 mM Tris HCl pH 7.5, EDTA 1mM and 0.5% NP40) supplemented with protease inhibitor, PMSF and phosphatase inhibitor. For ubiquitylation assays, cells were lysed with triple detergent buffer (150 mM NaCl, 1% NP40, 0.1% SDS, 50 mM Tris HCl pH 8, 0.5% NaDOC). The lysates were incubated overnight with the indicated antibodies for the immunoprecipitation. For pull down assay, lysates were incubated three hours with GST-fused proteins immobilized on glutathione beads. In both cases, pellets were washed three times with lysis buffer. Precipitates and 50 γ of whole cell lysates were loaded on SDS polyacrylamide gel and transferred on nitrocellulose membrane. Filter were blocked with 5% milk in TBS Tween 0.1%, incubated with primary and

secondary antibodies and finally proteins were detected with ECL (Euroclone).

Immunofluorescence and confocal analysis. Cells were plated on poly-D-lysine (Sigma) coated glass. Then cells were fixed with paraformaldehyde 5%, permeabilized with PBS 0.3% Triton, blocked with PBS 5% Bovine Serum Albumin (SERVA) and immunostained with the indicated primary antibody. Signals were revealed using secondary fluorescent antibodies (1:200; Invitrogen). Immunofluorescences were visualized using a Zeiss LSM 510 Meta argon/krypton laser scanning confocal microscope.

Real Time-RT PCR. Transcriptional levels of Sonic Hedgehog signalling pathway associated-genes in human samples were analysed by Real Time RT PCR. Total mRNA was extracted with TRIzol reagent (Sigma) according to the manufacturer protocol. 1µg of total mRNA from each sample was retrotranscribed using Luna Script RT SuperMix Kit (New England Biolabs). Real-Time PCR was performed using SYBR Green Master Mix (Biorad) using the following primers:

GLI2 5'-CAACGCCTACTCTCCCAGAC -3'
5'-GAGCCTTGATGTACTGTACCAC-3'

Each reaction was carried in triplicate using 25 ng of cDNA in 20µl. As internal control 18S ribosomal RNA expression levels were used. Melting curves were obtained by increasing the temperature from 60 to 95 °C with a temperature transition rate of 0.5 °C s^{-1}. Melting curves of final PCR products were analyzed (OpticonMonitor 3 Bio-Rad).

Medaka stocks. The Cab-strain of wild-type Medaka fish (Oryzias latipes) was maintained following standard conditions (i.e. 12 h/12 h dark/light conditions at 27°C). Embryos were staged according to (Avellino et al., 2013). All studies on fish were conducted in strict accordance with the Institutional Guidelines for animal research and approved by the Italian Ministry of Health; Department of Public Health, Animal Health, Nutrition and Food Safety in accordance to the

law on animal experimentation (D. Lgs. 26/2014). Furthermore, all animal treatments were reviewed and approved in advance by the Ethics Committee at the TIGEM Institute, (Pozzuoli, NA), Italy.

Sequence analysis. The available medaka Ol-TBC1D31 (ENSORLT00000007876.1) at chr16:11638220-11645068 genomic sequence was retrieved from public databases (http://genome-euro.ucsc.edu/) and aligned with human TBC1D31 transcript (ENST00000287380.6) to identify exons based on sequence.

mRNA and MO injection of medaka embryos. In vitro synthesis of human TBC1D31, wild-type OFD1, $OFD1_{S735A}$, $OFD1_{S735D}$ and hpraja2rm mRNAs were performed following manufacture's instruction (Porpora 2018). mRNAs were injected at 25-100 ng to observe dose-dependent phenotypes; selected working concentrations were 50 ng/μl for single injections and 25 ng/μl for combined injections. A morpholino (Mo; Gene Tools LLC, Oregon, USA) was designed against the splicing donor of exon 3 (Mo-Ol-TBC1D31: 5' -CACCAGACGAAATCTACTCCAAGTT-3') of the medaka orthologous of the TBC1D31 gene. Mo-Ol-TBC1D31 was injected at 0.15 mM concentration into one blastomere at the one/ two-cell stage. Off-target effects of the morpholino injections were excluded by repeated experiments with control morpholino or by co-injection with a p53 morpholino (Mo-p53: 5'-CGGGAATCG-CACCGACAACAATACG-3') as described (Porpora 2018).

Whole-mount immunostaining. Whole-mount immunostaining was performed and photographed, as described (Conte 2010). Embryos at Stage 24 were fixed in 4% paraformaldehyde, 2X phosphate-buffered saline (PBS) and 0.1% Tween-20. The fixed embryos were detached from chorion and washed with PTW 1X. Embryos were digested 7 minutes with 10 g/ml proteinase K and washed twofold with 2 mg/ml glycine/ PTW 1X. The samples were fixed 20 min in 4% paraformaldehyde, 2X phosphate-buffered saline (PBS) and 0.1% Tween-20, washed with PTW 1X and then incubated for 2 h in FBS 1%/PTW 1X, at room temperature. The embryos were incubated with mouse anti acetylated α -tubulin

antibody 1:400 (Sigma-Aldrich), overnight at 4°C. The samples were washed with PTW 1X, incubated with the secondary antibody, Alexa-488 goat anti-mouse IgG (Thermo Fisher), then with DAPI. Finally, the embryos were placed in glycerol 100%.

4. Results

4.1 TBC1D31 binds praja2 at residues 530-630.

By yeast two-hybrid screening using praja2 as a bait, I identified the C-terminal portion of TBC1D31 (aa 940-970) as prey. TBC1D31 is a protein localized at the centrosome with unknown function (Gupta 2015).

I first confirmed the interaction between TBC1D31 and praja2 by co-immunoprecipitation (Co-Ip) assays, using lysates of HEK293 cells transiently co-expressing GFP-TBC1D31 and flag-praja2 protein (**Fig. 10 A**). Then, I decided to identify the domain(s) of praja2 that binds TBC1D31. To this aim, I performed Co-Ip assays using cells expressing GFP-TBC1D31 and the following flag-tagged deletion mutants of praja2: 1-530, 1-630 and a mutant that lacks only the residues from 530 to 630 (Δ530-630). The analysis identified the residues 530-630 of praja2 as the binding site for TBC1D31 (**Fig. 10 B and C**).

I confirmed the interaction *in vitro* between praja2 and TBC1D31 by pull-down assay using a GST protein fused to residues 530-630 of praja2 and lysates from HEK293 cells expressing GFP-TBC1D31 (**Fig. 10 D**).

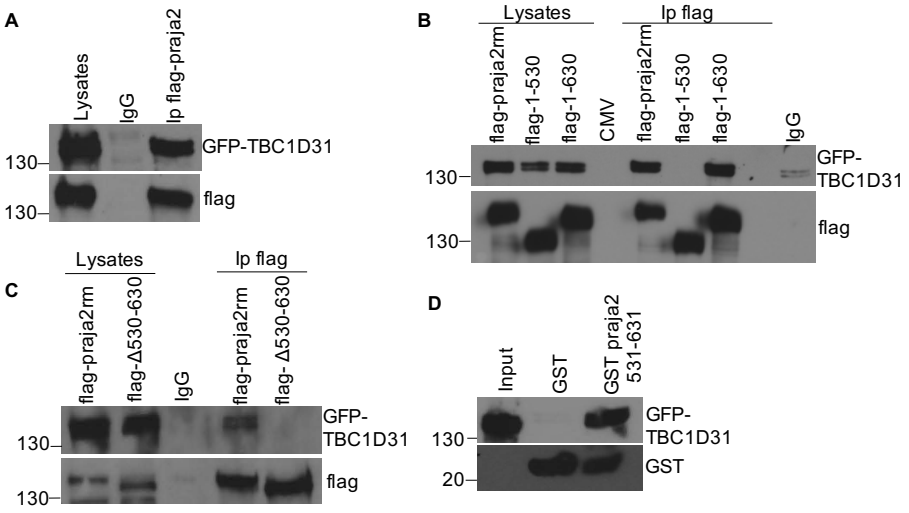

Figure 10. TBC1D31 binds praja2 at residues 530-630. A. Lysates were immunoprecipitated with anti-flag antibody or control IgG and then precipitates and a quote of lysates were immunoblotted with anti-GFP and anti-flag antibodies. **B.** HEK293 cells were co-transfected with GFP-TBC1D31 and flag-praja2 vectors (praja2rm, praja2$_{1-530}$, praja2$_{1-630}$). Lysates were immunoprecipitated with anti-flag antibody or control IgG. Precipitates and a quote of lysates were immunoblotted with anti-GFP and anti-flag antibodies. **C.** HEK293 cells were co-transfected with GFP-TBC1D31 and flag-praja2 vectors (praja2rm or praja2$_{\Delta 530-630}$). Lysates were immunoprecipitated with anti-flag antibody or control IgG. Precipitates and a quote of lysates were immunoblotted with anti-GFP and anti-flag antibodies. **D.** HEK293 cells were transfected with GFP-TBC1D31. Lysates were subjected to pull-down with GST and GST-praja2$_{531-631}$. Precipitates and a quote of lysates were immunoblotted with anti-GFP and anti-GST antibodies.

The domain of TBC1D31 from 940 to 970 was identified in the two-hybrid screening as the prey that interacts to praja2 bait. I confirmed this interaction in vitro performing a pull-down assay using a GST protein fused to residues 940 to 970 of TBC1D31 protein and lysates derived from cells expressing flag-praja2 (**Fig. 12**).

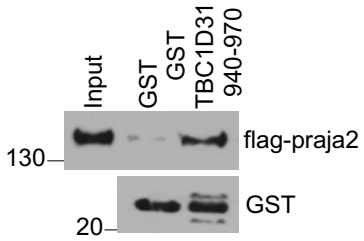

Figure 11. TBC1D31 940-970 residues bind praja2 in vitro. HEK293 cells were transfected with flag-praja2. Lysates were subjected to pull-down with GST and GST-TBC1D31$_{940\text{-}970}$. Precipitates and a quote of lysates were immunoblotted with anti-flag and anti-GST antibodies.

praja2 acts as an AKAP that targets PKA at specific cellular compartments (Lignitto 2011). For this reason, I investigated the presence of PKA in the TBC1D31/praja2 complex. Immunoprecipitation of TBC1D31 from HEK293 cell lysates allowed the recovery of a trimeric complex containing TBC1D31, praja2 and the catalytic subunit of PKA (PKAc) (**Fig. 12**).

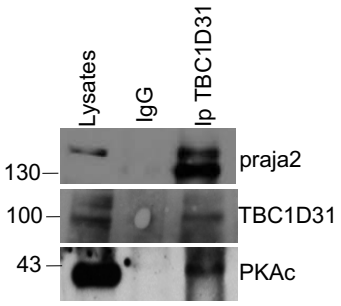

Figure 12. TBC1D31, praja2 and PKAc form a trimeric complex. HEK293 lysates were immunoprecipitated with anti-TBC1D31 antibody or control IgG. Precipitates and a quote of lysates were immunoblotted with anti-praja2, anti-TBC1D31 and anti-PKAc antibodies.

4.2 TBC1D31 targets praja2 at the centrosome

TBC1D31 was identified as a protein localized at the centrosome/basal body (Gupta et al, 2015). I confirmed the localization of TBC1D31 at the centrosome in HEK293 cells by double immunofluorescence analysis using antibodies against TBC1D31 and γ-tubulin, a marker of the centrosome. **Fig.13A** shows that TBC1D31 is localized at the centrosome and centriolar satellites. Similarly, I found that praja2 localized at the centrosome (**Fig. 13B**). I confirmed colocalization of both proteins, praja2 and TBC1D31, at the centrosome. Thus, TBC1D31 and praja2 colocalize, at least in part, within the same intracellular compartment (**Fig. 13C**).

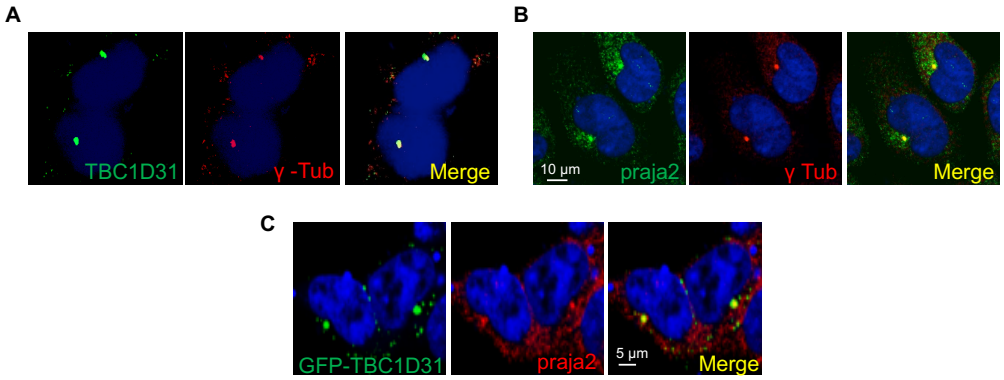

Figure 13. TBC1D31 and praja2 colocalize within the centrosome. A. HEK293 cells were fixed and stained for TBC1D31, γ-tubulin and DRAQ5. **B.** HEK293 cells were fixed and stained for praja2, γ-tubulin and DRAQ5. **C.** HEK293 cells expressing GFP-TBC1D31 were fixed and stained for praja2 and DRAQ5.

Then, I asked if TBC1D31 targets praja2 at the centrosome. By immunofluorescence analysis in HEK293 cells, I found that genetic silencing of TBC1D31 dramatically reduced the levels of praja2 staining at the centrosome, compared to control cells, supporting the notion that TBC1D31 acts as an anchor for praja2 (**Fig. 14A**). TBC1D31 silencing was confirmed by western blot analysis (**Fig. 14B**).

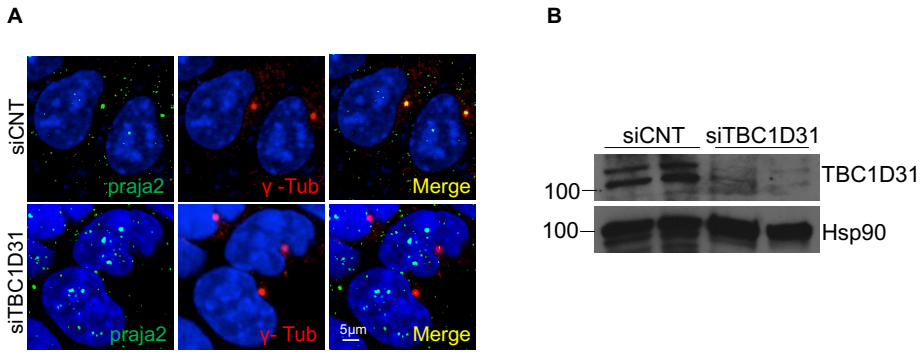

Figure 14. TBC1D31 targets praja2 at centrosome. A. HEK293 cells transfected with control siRNA or siRNA targeting endogenous TBC1D31 were fixed and stained for praja2, γ-tubulin and DRAQ5. **B.** Immunoblot analysis of TBC1D31 and Hsp90 in TBC1D31 silenced cells.

4.3 OFD1 is a component of the praja2/TBC1D31 complex

OFD1 is a protein localized at the centrosome/basal body and at the centriolar satellites and plays an important role in cilium biology. OFD1 takes part of a PKA in a variety of normal and cancer cells (Rinaldi 2019). Accordingly, I decided to tested the presence of OFD1 in the TBC1D31/praja2/PKA complex. A Co-Ip assay performed on lysates of HEK293 cells expressing GFP-TBC1D31 and flag-OFD1 demonstrated that OFD1 interacts with TBC1D31 and praja2 (**Fig. 15A**). Co-Ip assays on lysates derived from brain tissues demonstrated the existence of an endogenous complex composed of praja2/TBC1D31/OFD1 (**Fig. 15B**). Moreover, triple immunofluorescence assays in HEK293 cells transfected with GFP-TBC1D31 and flag-OFD1 confirmed the presence of a TBC1D31/praja2/OFD1 complex located within the same intracellular compartment (**Fig. 15C**).

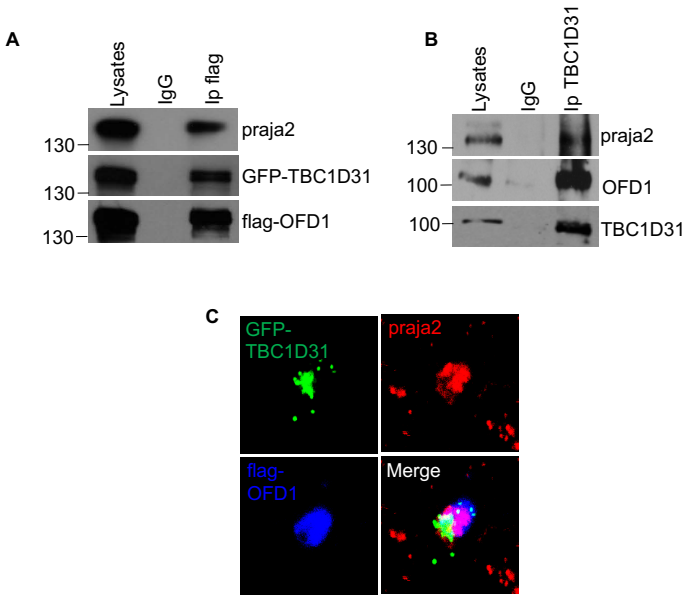

Figure 15. OFD1 interacts with TBC1D31/praja2 complex. A. Lysates of HEK293 cells co-transfected with GFP-TBC1D31 and flag-OFD1 were immunoprecipitated with anti-flag antibody or control IgG. Precipitates and a quote of lysates were immunoblotted with anti-praja2, anti-GFP and anti-flag antibodies. **B.** Lysates from mouse brain tissue were immunoprecipitated with anti-TBC1D31 antibody. Precipitates and a quote of lysates were immunoblotted with anti-praja2, anti-OFD1 and anti-TBC1D31 antibodies. **C.** HEK293 cells expressing GFP-TBC1D31 and flag-OFD1 were fixed and stained for flag and praja2.

4.4 PKA phosphorylates OFD1

OFD1, TBC1D31 and praja2 form a complex that includes PKA, the main effector of cAMP. Thus, I decided to investigate the cAMP mediated regulation of the complex. I tested OFD1 phosphorylation in HEK293 cells expressing flag-OFD1, serum deprived for 24 hours and then treated for 1 hour with Forskolin (FSK), a diterpene that raises cAMP levels. Using phospho-PKA substrates antibodies, I found that cAMP induced a marked phosphorylation of OFD1 (**Fig.16 A and B**). A prediction analysis of OFD1 protein sequence identified

two putative PKA consensus residues (S735 and S899), but only S735 was conserved in the mouse variant (S739) (**Fig. 16C**). Accordingly, I generated an OFD1 mutant carrying S735 substituted with alanine (OFD1 S735A). FSK stimulation failed to induce phosphorylation of OFD1 S735A mutant (**Fig 16 A and B**), compared to wild type protein. This finding indicates that serine 735 contributes to the overall OFD1 phosphorylation induced by cAMP. To prove that OFD1 phosphorylation was mediated by PKA, I replicated the phosphorylation assay pretreating cells with H89, an inhibitor of PKA. **Fig 16 A and B** show that pre-treatment with H89 completely abrogated cAMP-mediated OFD1 phosphorylation.

These results demonstrated that PKA phosphorylates OFD1 at S735 in cells.

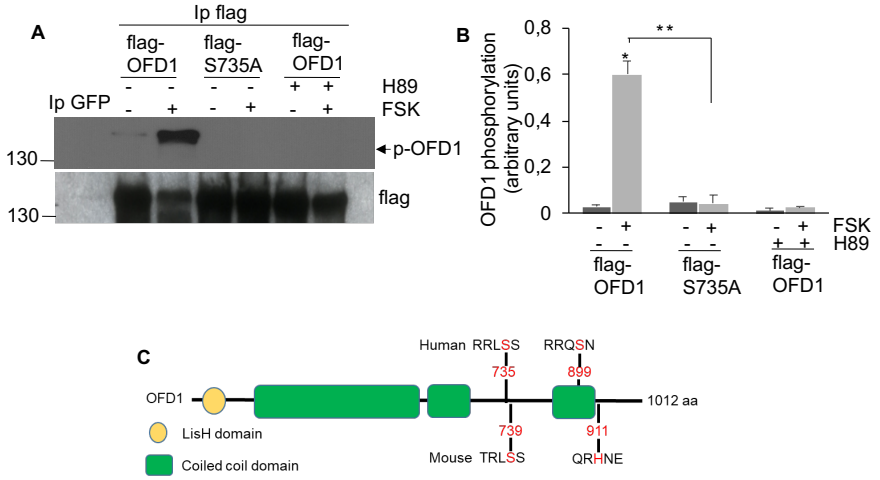

Figure 16. PKA phosphorylates OFD1 at the serine 735. A. HEK293 were transfected with flag-OFD1 or flag-S735A vectors, serum deprived for 24 hours and then treated with forskolin (FSK) (40 μM) for 1 hour. Where indicated, cells were pretreated with H89 (10 μM) for 30 minutes. Lysates were immunoprecipitated with anti-flag antibody or GFP antibody as control. Precipitates were immunoblotted with anti-flag and anti-phospho-(K/R)(K/R)X(S*/T*) antibodies. **B.** Quantitative analysis of three independent experiments shown in A. Student's t test *p<0,05, **p<0,01. **C.** Schematic representation of OFD1 domain organization, with predicted phosphorylation sites at S735 and S899 in human variant.

Previous report demonstrated that praja2 acts as an AKAP that binds and targets PKA to specific intracellular compartments (Lignitto 2011). Considering that I demonstrated the presence of praja2 in complex with OFD1, PKA and TBC1D31, I decided to investigate whether praja2 allowed PKA-mediated phosphorylation of OFD1 within the complex. I tested this hypothesis by monitoring OFD1 phosphorylation in cells subjected to genetic silencing of praja2. **Fig. 17 A and B** show that, in absence of praja2, cAMP mediated phosphorylation of OFD1 is drastically reduced, supporting the hypothesis that the phosphorylation of OFD1 occurs within the praja2/TBC1D31 complex.

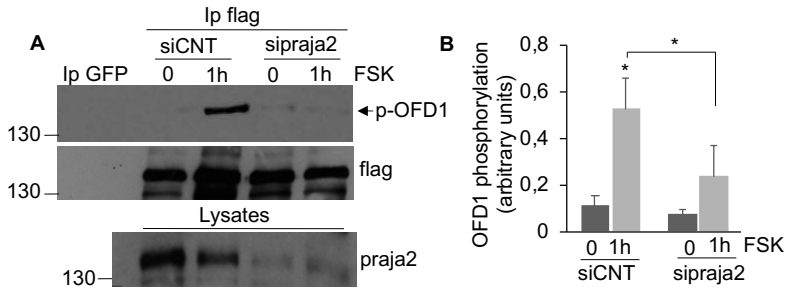

Figure 17. praja2 is necessary for PKA-mediated OFD1 phosphorylation. A. HEK293 co-transfected with flag-OFD1 and control siRNA or siRNA targeting endogenous praja2, were serum deprived for 24 hours and treated with FSK (40 μM) for 1 hour. Lysates were immunoprecipitated with anti-flag antibody and anti-GFP antibody as control. Precipitates were immunoblotted with anti-phospho-(K/R)(K/R)X(S*/T*) PKA substrates and anti-flag antibodies. A quote of lysates was immunoblotted with anti-praja2 antibody. **B**. Quantitative analysis of experiment shown in A. A mean of three independent experiments is shown. *p<0,05.

4.5 cAMP primes OFD1 to praja2-mediated ubiquitylation and proteolysis. praja2 is an E3 ubiquitin ligase regulated by cAMP and is present in complex with OFD1. Thus, I tested whether praja2 ubiquitylates OFD1. Ubiquitylation assays were performed in HEK293 cells overexpressing myc-OFD1, ubiquitin-HA and either flag-praja2 wild-type or flag-praja2 ring mutant (praja2rm), that binds substrates but is unable to transfer ubiquitin to them. **Fig. 18A** shows that OFD1 was heavily polyubiquitylated by praja2. Conversely, the ubiquitylation of OFD1 was abrogated in the presence of praja2rm.

Next, I tested OFD1 ubiquitylation in cAMP-stimulated HEK293 cells. FSK treatment in cells overexpressing flag-OFD1 and ubiquitin-HA induced a markedly polyubiquitylation of OFD1 that was almost reversed by genetic silencing of praja2 (**Fig. 18B**), supporting the hypothesis that cAMP induces OFD1 ubiquitylation through praja2.

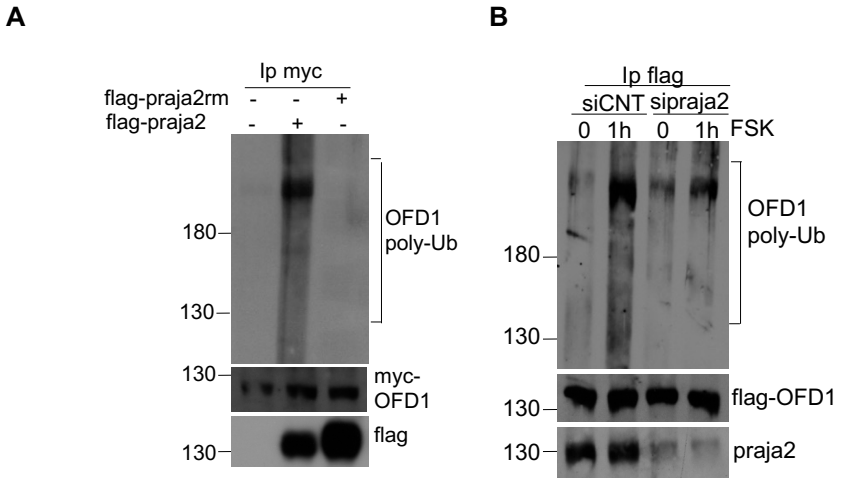

Figure 18. cAMP induces praja2-mediated OFD1 ubiquitylation. A. HEK293 were co-transfected with myc-OFD1, ubiquitin-HA and flag-praja2 either wild-type or ring mutant (praja2rm). Lysates were immunoprecipitated with anti-myc antibody. Precipitates were immunoblotted with anti-myc and anti-HA antibodies, lysates were immunoblotted with anti-flag antibody. **B.** HEK293 co-transfected with flag-OFD1, ubiquitin-HA and either control siRNA or siRNA targeting endogenous praja2, were immunoprecipitated with anti-flag antibody. Precipitates were immunoblotted with anti-flag and anti-HA antibodies; lysates were immunoblotted with anti-praja2 antibody.

Ubiquitylation is often coupled to degradation of substrates. Hence, I tested whether cAMP induces also OFD1 proteolysis. First, I evaluated OFD1 half-life in HEK293 cells serum deprived for 24 hours and treated for different times with cycloheximide (CHX), an inhibitor of protein synthesis. **Fig. 19A** shows that CHX treatment didn't affect OFD1 levels. Instead, FSK treatment in cells treated with CHX induced a time dependent decline of OFD1 levels (**Fig. 19 A and B**). Furthermore, pretreatment of HEK293 cells with MG132, a proteasome inhibitor, completely reversed the time-dependent decline of OFD1 levels induced by cAMP stimulation, indicating that ubiquitylated protein is degraded via proteasome (**Fig. 19 C and D**). To prove that OFD1 proteolysis was mediated by praja2, I analyzed OFD1 levels in cells subjected to genetic silencing for praja2. Following transfection, cells were serum deprived overnight and then treated with FSK. **Fig. 19 E and F** show that downregulation of praja2 prevented OFD1 decline in cAMP-stimulated cells, compared to controls.

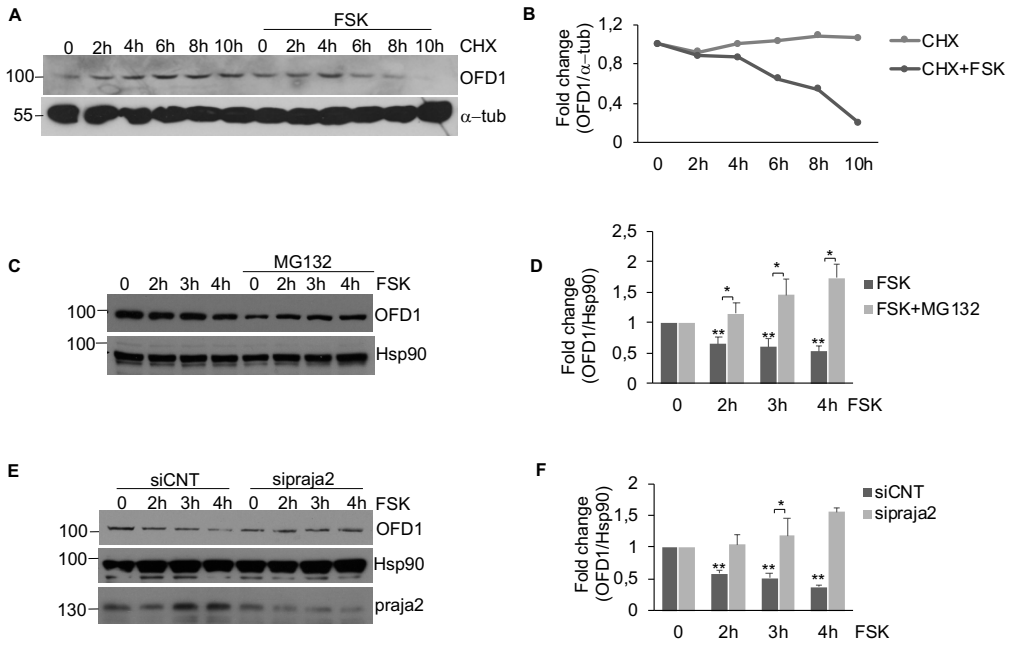

Figure 19. cAMP induces OFD1 proteolysis mediated by praja2. A. HEK293 serum deprived for 24 hours, were pretreated with cycloheximide (CHX) (100 μM) and, were indicated, treated with FSK (40 μM) for the indicated time points. Lysates were immunoblotted with anti-OFD1 and anti-α-tubulin antibodies. **B.** Quantitative analysis of experiments shown in A. A mean of two independent experiments is shown. **C.** HEK293 serum deprived for 24 hours, were pretreated with MG132 (10 μM) and then with FSK (40 μM) for the indicated time points. Lysates were immunoblotted with anti-OFD1 and anti-Hsp90 antibodies. **D.** Statistical analysis of experiments shown in A. A mean of three independent experiments is shown. Student's t test *p<0,05 **<0,01. **E.** HEK293 transfected with control siRNA or siRNA targeting endogenous praja2, were serum deprived for 24 hours, pretreated with CHX (100 μM) for 30 minutes and then treated with FSK (40 μM) for the indicated time points. Lysates were immunoblotted with anti-OFD1, anti-praja2 and anti-Hsp90 antibodies. **F.** Statistical analysis of experiments shown in A. A mean of three independent experiments is shown. Student's t test *p<0,05 **<0,01.

4.6 Phosphorylation primes OFD1 to ubiquitylation and proteolysis

Next, I tested whether OFD1 phosphorylation by PKA at S735 was required for its ubiquitylation and proteolysis. To this end, I performed ubiquitylation assays

in cells overexpressing ubiquitin-HA and either flag-OFD1 or flag-S735A mutant. Following transfection, cells were serum deprived for 24 hours and then treated with FSK. **Fig. 20A** shows that ubiquitylation of OFD1 mutant induced by FSK treatment was completely abrogated, compared to OFD1 wild-type variant.

Next, I evaluated OFD1 proteolysis in cells expressing S735A mutant. As expected, cAMP stimulation was unable to affect the levels of S735A mutant, compared to wild-type protein (**Fig. 20 B and C**). These experiments demonstrate that phosphorylation is a prerequisite for OFD1 ubiquitylation and proteolysis mediated by praja2-UPS pathway.

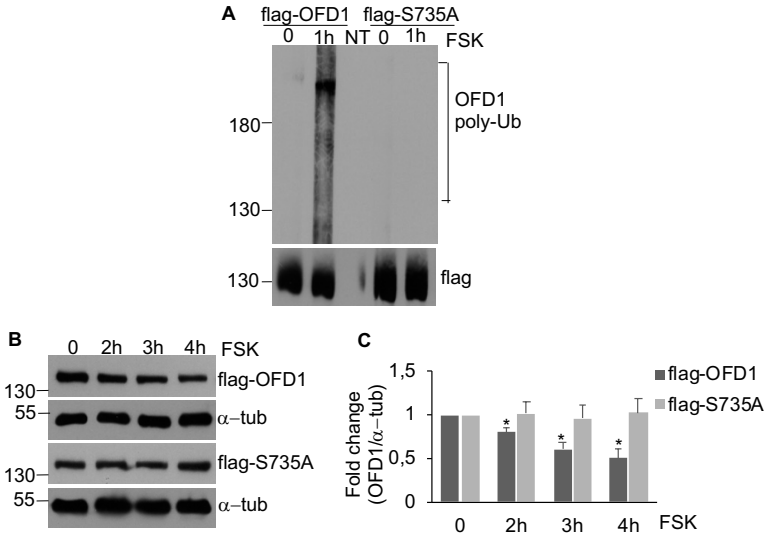

Figure 20. OFD1 phosphorylation induces its ubiquitylation and proteolysis. A. HEK293 co-transfected with ubiquitin-HA and either flag-OFD1 or flag-S735A, were serum deprived for 24 hours and treated for 1 hours with FSK (40 μM). Lysates were immunoprecipitated with anti-flag antibody. Precipitates were immunoblotted with anti-HA and anti-flag antibodies. **B.** HEK293 transfected with flag-OFD1 or flag-S735A, were serum deprived for 24 hours, pretreated with CHX (100 μM) for 30 minutes and treated with FSK (40 μM) for the indicated time points. Lysates were immunoblotted with anti-flag and anti-α-tubulin antibodies. **C.** Statistical analysis of experiments shown in A. A mean of three independent experiments is shown. Student's t test *p<0,05.

The Oro-Facial Digital type I syndrome is caused by mutations of OFD1 gene. More than 130 different mutations were identified and about 30% of them are point mutation (Macca 2009; Romio 2003). Mutations occurring in LisH domain are related to alteration of OFD1 function in ciliogenesis (Singla et al, 2010). The OFD1 E97G mutation is one of the most mutated residues within the LisH domain (Macca 2009). I decided to investigate the effect of cAMP stimulation on the mutant form of OFD1. **Fig. 21 A and B** show that OFD1 E97G levels weren't affected by FSK treatment, suggesting a pathogenic role of altered proteolysis of OFD1 in this ciliopathy disorder.

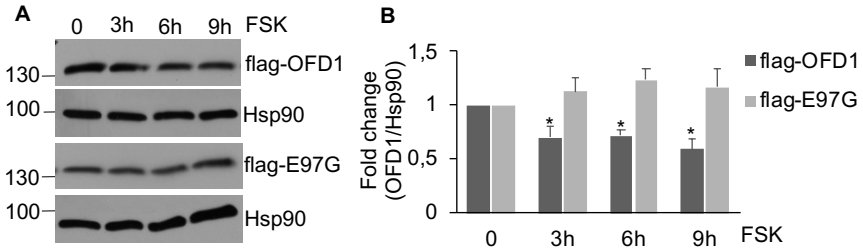

Figure 21. OFD1 E97G has an altered proteolysis. A. HEK293 transfected with flag-OFD1 or flag-E97G, were serum deprived for 24 hours, pretreated with CHX (100 μM) for 30 minutes and treated with FSK (40 μM) for the indicated time points. Lysates were immunoblotted with anti-flag and anti-Hsp90 antibodies. **B.** Statistical analysis of experiments shown in A. A mean of three independent experiments is shown. Student's t test *p<0,05.

4.7 TBC1D31/OFD1/praja2/PKA axis regulates ciliogenesis

Ciliogenesis is a finely regulated process that occurs under growth arrest condition, when the mother centriole of the centrosome migrates under the plasma membrane, differentiates into a basal body and starts to elongate as an axonemal structure. Given the peculiar localization of TBC1D31 at the centrosome and the role of centrosome in primary ciliogenesis, I tested the localization of TBC1D31 in ciliated cells. To this end, HEK293 cells were serum deprived for 48 hours to induce cilia formation, and then stained for acetylated α–tubulin, a modified form of tubulin that accumulates at the ciliary axoneme.

As expected, TBC1D31 was localized at the basal body of primary cilium (**Fig. 22A**).

I evaluated also whether TBC1D31 was necessary for cilia formation. **Fig. 22 B and C** show that genetic silencing of TBC1D31 drastically reduced the percentage of ciliated cells, compared to control cells. This finding suggested an important role of TBC1D31 in primary ciliogenesis.

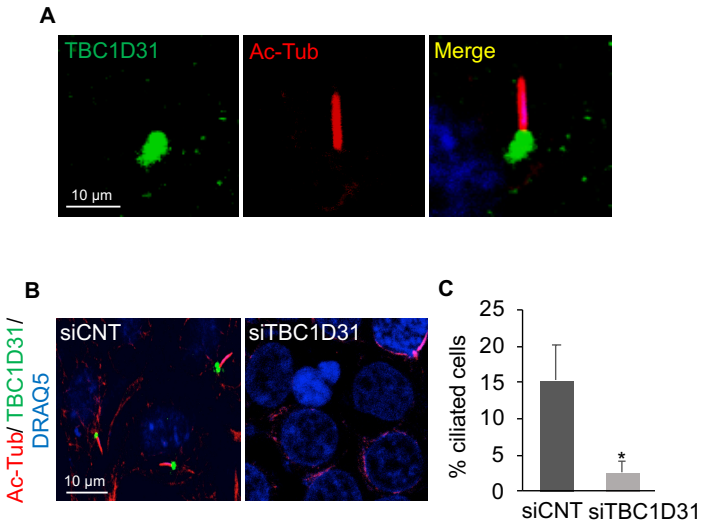

Figure 22. TBC1D31 localized at the basal body of primary cilia and it is necessary for primary ciliogenesis. A. HEK293 were serum deprived for 48 hours, fixed and stained for TBC1D31 and acetylated α-tubulin. **B.** HEK293 cells transfected with control siRNA or siRNA targeting endogenous TBC1D31 were serum deprived for 48 hours, fixed and stained for TBC1D31 and acetylated α-tubulin. **C.** Quantitative analysis of experiments shown in A. A mean of four independent experiments is shown. Student's t test *p<0,05.

The data above indicate that OFD1 stability is regulated by the PKA-cAMP signaling. Considering the role of OFD1 in primary ciliogenesis, I investigated whether regulation of OFD1 by PKA might impact on primary cilia formation. HEK293 cells were transiently transfected either with flag-OFD1 or flag-S735A mutant and serum-deprived for 48 hours to induce cilia formation. Staining for α-acetylated-tubulin shows that morphology of primary cilia was markedly

altered in cells expressing OFD1-S735A mutant with fragmentation and interruptions along the axoneme (**Fig. 23 A upper panels and B**). No significant changes of cilium morphology were evident in cells expressing the wild type variant. The number of ciliated cells was not modified by OFD1 or S735A expression (**Fig. 23 C**). The same cilia alterations were observed also in cells expressing cilia-APEX-GFP, a cilia-targeted proximity labeling enzyme (**Fig. 23 A middle panels**). Moreover, the staining for ARL13B, a protein localized at the ciliary membrane, showed similar results in NIH3T3 cells (**Fig. 23 A lower panels**).

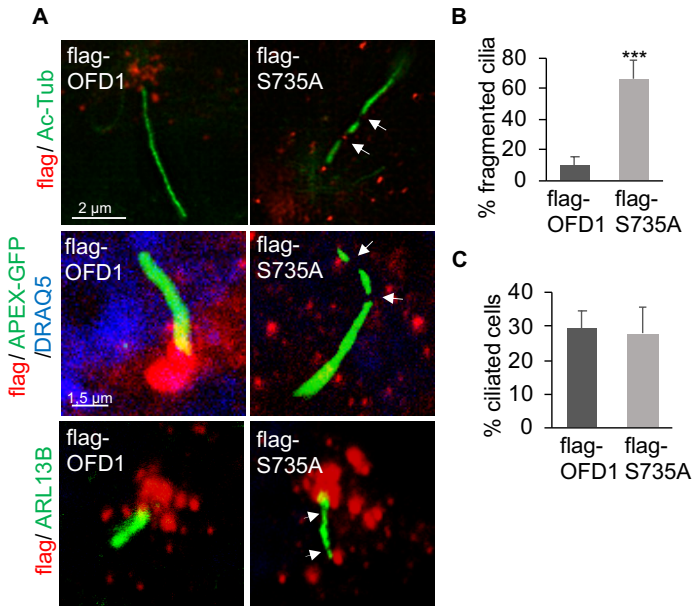

Figure 23. OFD1 phosphorylation controls cilium morphology. A. HEK293 cells transfected with flag-OFD1 or flag-S735A were serum deprived for 48 hours, fixed and stained for flag and acetylated α-tubulin. Where indicated cells were co-transfected with cilia-APEX-GFP (middle panel). In lower panels, NIH3T3 cells expressing either flag-OFD1 or S735A-flag were serum deprived for 48 hours, fixed and stained for flag and ARL13B. **B-C** Quantitative analysis of experiments shown in A. A mean value of three independent experiments is shown. Student's t test ***p<0,001.

cAMP-PKA signaling plays a key role in inducing cilia resorption in serum-deprived cells (Porpora 2018). Accordingly, I tested the effect of OFD1 phosphorylation by PKA in cilium disassembly. HEK293 cells, expressing either an empty vector (NT), flag-OFD1 or flag-S735A were serum deprived for 48 hours and treated 6 hours with FSK. In control cells and in OFD1-expressing cells, cAMP induced a reduction of the percentage of ciliated cells; conversely, in cells expressing the phosphorylation mutant of OFD1, the treatment with FSK had no major impact on the percentage of ciliated cells (**Fig. 24 A and B**). These results indicate that OFD1 phosphorylation by PKA plays an important role in cilia morphology and dynamics.

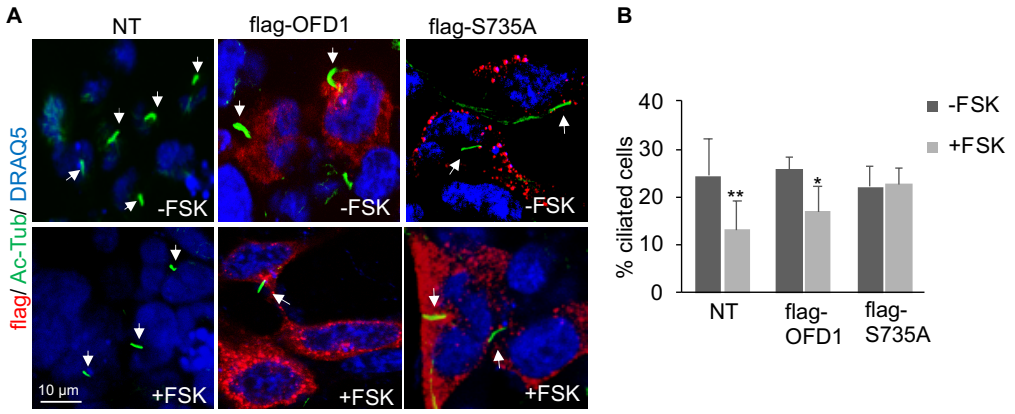

Figure 24. OFD1 phosphorylation controls ciliogenesis. A. HEK293 cells transfected with flag-OFD1 or flag-S735A were serum deprived for 48 hours and treated with FSK (40 µM) for 6 hours. Cells were fixed and stained for flag, acetylated α-tubulin and DRAQ5. **B.** Quantitative analysis of experiments shown in A. A mean value of three independent experiments is shown. Student's t test *p<0,05 **p<0,01.

Activation of cAMP-PKA signaling in the ciliary compartment inhibits Sonic Hedgehog pathway (Tempé 2006). I decided to investigate if PKA-mediated OFD1 phosphorylation had a role in this pathway. To this end, I used NIH3T3 cells transiently expressing either empty vector, flag-OFD1 or flag-S735A. Following transfection, cells were serum deprived and treated with purmorphamine (agonist of Smoothened), alone or in combination with FSK. I

evaluated mRNA levels of gli2 as readout of SHH pathway activation. **Fig. 25** shows that, in control cells and in cells expressing OFD1 wild-type, purmorphamine treatment induced high levels of gli2 mRNA. In these cells, treatment with FSK prevented gli2 mRNA accumulation. In contrast, expression of the S735A mutant completely abolished gli2 mRNA accumulation in purmorphamine-treated cells (**Fig. 25**). These results support the hypothesis that OFD1 phosphorylation plays an important role in the SHH signaling pathway.

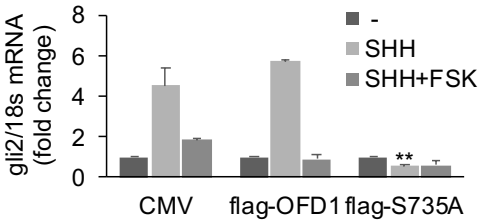

Figure 25. OFD1 phosphorylation controls SHH signaling. NIH3T3 cells expressing either empty vector (CMV), flag-OFD1 or flag-S735A, were serum deprived for 24 hours and treated for 24 hours with purmorphamine (SHH). Where indicated cells were treated with FSK (40 μM) for 6 hours. gli2 RNA was analyzed by quantitative pcr with reverse transcription. A mean value of three independent experiments is shown. Student's t test **p<0,01.

4.8 TBC1D31/OFD1/praja2/PKA axis regulates Medaka fish development

To prove the role of TBC1D31, which is conserved among vertebrates, in the ciliogenesis *in vivo*, we carried out an *in vivo* analysis in the Medaka fish (Oryzias latipes, Ol) model system using gene knockdown, gene overexpression and rescue experiments. A Morpholino (Mo) against TBC1D31 was designed and injected in Medaka embryos (Ol-TBC1D31 KD). From stage 24, silencing of TBC1D31 caused a delay in development, with morphological alteration associated with microcephaly, microphthalmia, pigmentation defects and pericardial edema (**Fig 26 A**). To teste whether these abnormalities were

associated with alteration in primary ciliogenesis, immunofluorescence assays were performed in the apical surface of neural tube cells of Medaka embryos stained with acetylated α-tubulin. **Fig 26 B and C** show that the length of primary cilia in Ol-TBC1D31 KD was drastically reduced compared to wild-type embryos. To prove that this phenotype was specifically due to the absence of TBC1D31, TBC1D31 mRNA was injected in Ol-TBC1D31 KD. **Fig 26 A-C** show that injection of TBC1D31 completely rescued the length of primary cilia and consequently also embryos phenotype, indicating that TBC1D31 has a fundamental role in Medaka fish development. I demonstrated that PKA-phosphorylation of OFD1 in the TBC1D31 assembled complex plays a fundamental role in the regulation of primary cilia. Hence, I decided to evaluate the effects of S735A mutant in Medaka fish development. **Fig. 26 A** shows that Medaka embryos injected with S735A mRNA had a similar phenotype to Ol-TBC1D31 KD. Alterations in the development were related to defects in ciliogenesis that generate highly fragmented cilia (**Fig. 26 B and C**). The cilia length in OFD1-injected Medaka embryos was evaluated. As expected, ciliogenesis was similar to wild-type embryos (**Fig. 26 B and C**). These results confirmed that OFD1 phosphorylation played an important role in ciliogenesis and also in Medaka fish development.

If most of the changes in the ciliogenesis caused by Ol-TBC1D31 KD are due to altered phosphorylation and proteolysis of OFD1 by praja2 activity, I reasoned that co-injection of $OFD1_{S735D}$ mutant, mimicking OFD1 phosphorylated form, combined with the dominant negative variant of human praja2 (hpraja2rm), should re-establish, at least in part, the ciliogenesis in Mo-Ol-TBC1D31 morphants and rescue larva phenotype. **Fig. 26 A** shows that co-injection of S735D/praja2rm mRNA in Ol-TBC1D31 KD completely rescued the whole embryos phenotype. Cilia length of Ol-TBC1D31 KD injected with S735D/praja2rm mRNA was rescued by about 50% (**Fig. 26 B and C**). As control, either OFD1 wild-type or OFD1 S735A mutant were injected in Ol-

TBC1D31 KD and, as expected, no rescue was observed neither in Medaka phenotype nor in cilia length (**Fig. 26 A-C**).

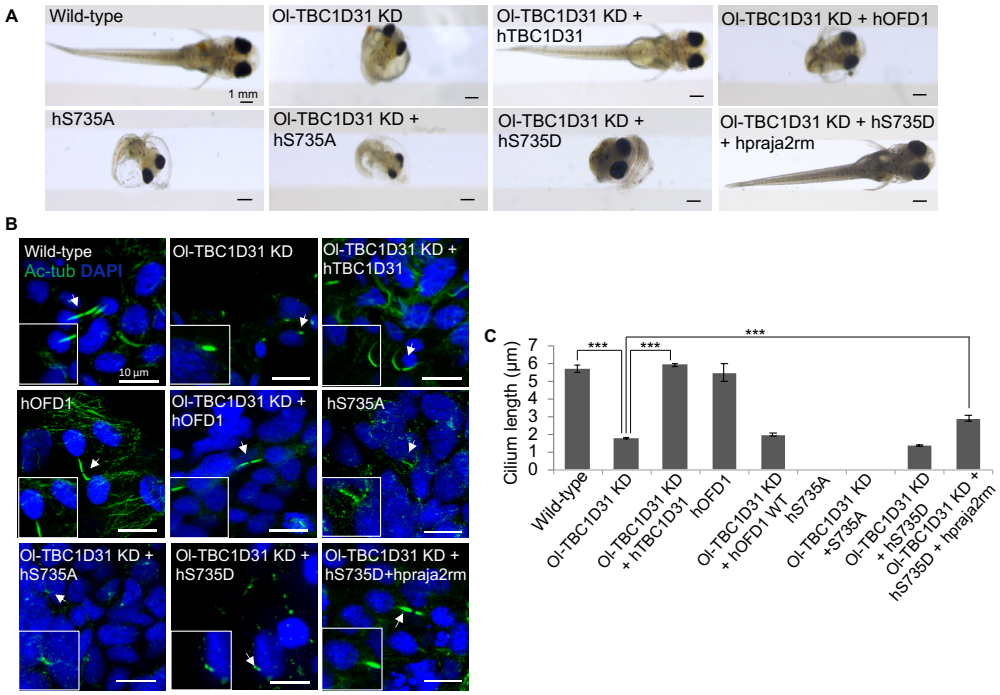

Figure 26. TBC1D31 and OFD1/praja2/PKA axis regulates Medaka fish development

A. Stereomicroscopic images of WT, Ol-TBC1D31 KD, Ol-TBC1D31 KD + hTBC1D31, Ol-TBC1D31 KD + hOFD1 WT, hS735A, Ol-TBC1D31 KD + hS735A, Ol-TBC1D31KD + hS735D and Ol-TBC1D31 KD + hS735D + hpraja2 rm injected Medaka larvae, at stage 40. **B.** Confocal images of cilia of the neural tube cells in the wild-type, Ol-TBC1D31 KD, Ol-TBC1D31 KD + hTBC1D31, hOFD1, Ol-TBC1D31 KD + hOFD1, hS735A, Ol-TBC1D31 KD + hS735A, Ol-TBC1D31 KD+ hS735D and Ol-TBC1D31 KD + hs735D + hpraja2rm stained for acetylated α-tubulin Ab (green) and DAPI (blue). **C.** Quantitative analysis of experiments shown in B. Cilium length was analyzed. Student's t test ***p<0,001.

The specificity of injected mRNA was evaluated by western blot analysis performed in Medaka embryos tissues (**Fig. 27 A and B).**

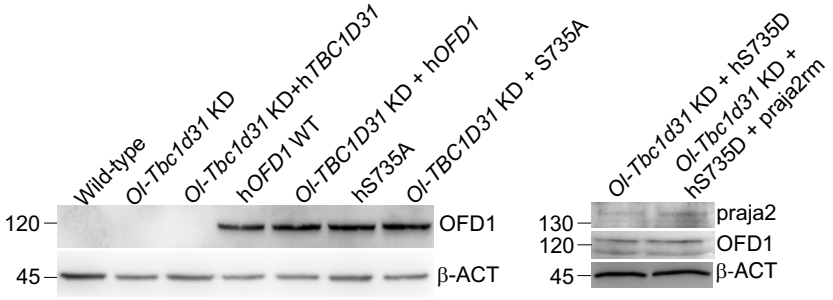

Figure 27. Human protein expression in Medaka fish tissues. A. Representative immunoblots of OFD1 and β-actin from indicated Medaka embryos. **B.** Representative immunoblots of praja2, OFD1 and β-actin from indicated Medaka embryos.

These results strongly support the hypothesis that phosphorylation and ubiquitin-dependent proteolysis of OFD1 within the TBC1D31 complex is fundamental for ciliogenesis and Medaka fish development.

5. Discussion

In my PhD thesis, I described the presence of a TBC1D31 complex at the centrosome that includes praja2, OFD1 and PKA. cAMP signaling regulates this complex, inducing OFD1 phosphorylation by colocalized PKA and its ubiquitylation and proteolysis through praja2-UPS pathway. This mechanism has a fundamental role in promoting primary cilium disassembly.

In the laboratory where I performed these studies, the RING-H2 E3 ligase praja2 has been extensively studied. By yeast two-hybrid screening performed using praja2 as a bait, I identified TBC1D31 as praja2 interactor. TBC1D31 is a protein recently identified as a component of the centrosome and also of the ciliary compartment, but its function was largely unknown (Gupta 2015). By CoIp and *in vitro* binding assays, I identified the aminoacidic residues 530-630 of praja2 as the binding site of TBC1D31. Moreover, I confirmed that the C-terminal portion of TBC1D31 is responsible for direct binding to praja2.

I demonstrated that TBC1D31 and praja2 complex is localized at the centrosome. TBC1D31 acts as an anchor for praja2 at the centrosome. The centrosome plays a fundamental role in primary ciliogenesis. When cells exit the mitotic cycle, the centrosome is rearranged in the basal body of cilia (Sánchez 2016). Accordingly, functional analysis demonstrated that TBC1D31 plays an essential role in primary ciliogenesis. Praja2 is an AKAP that targets PKA at specific cellular compartment, near its substrates, controlling cAMP signaling at discrete intracellular compartments (Lignitto 2011). Hence, I found that PKA was also present in the TBC1D31 complex. These findings suggest a role of TBC1D31/praja2/PKA complex in primary ciliogenesis.

OFD1 was identified as a member of the TBC1D31 assembled complex. Within the complex, OFD1 is phosphorylated by PKA at serine 735. Phosphorylation of OFD1 was completely abrogated by praja2 silencing, confirming that praja2 acts as an AKAP that locally facilitates OFD1 phosphorylation at the centrosome. OFD1 phosphorylation was essential for its ubiquitylation by praja2. I identified a centrosome-based transduction unit that controls PKA-mediated

phosphorylation of OFD1 and ubiquitylation by colocalized praja2. For the first time, I report a regulation of OFD1 by the praja2-UPS system in response to cAMP signaling. By removing OFD1, praja2 controls primary ciliogenesis. UPS is involved in the dynamic regulation of primary cilia structure and function, through the control of protein turnover of key ciliary elements involved both in the assembly and disassembly of primary cilia (Hossain 2019). The cAMP-mediated proteolysis of OFD1 by praja2 induces cilia disassembly and downregulation of signaling in the ciliary compartment.

The role of OFD1 in primary ciliogenesis is still debated. OFD1 is localized at the centrosome and pericentriolar satellites, and it was identified as a ciliary protein located at the basal body. Thus, mutations of OFD1 gene are responsible of a ciliopathy known as Oro-Facial Digital syndrome (Ferrante 2001). The removal of OFD1 portion located at pericentriolar satellites is essential for the initial step of primary ciliogenesis. Pericentriolar OFD1 binds BBS4, a component of the BBSome complex. BBSome is essential for the regulation of the IFT complex and for the transport of ciliary membrane proteins in the ciliary compartment; thus, mutations in BBSome components are associated with Bardet-Biedel syndrome, one of the best-known ciliopathies (Wingfield 2017).

In growing conditions, OFD1 retains BBS4, thereby inhibiting the onset of primary cilia. Following serum deprivation, pericentriolar OFD1 is actively removed by the autophagy machinery determining the release of BBS4 and the formation of primary cilia (Tang 2013). Conversely, the portion of OFD1 located at the centrosome is essential for primary ciliogenesis. Centriolar OFD1 is involved in the formation of distal appendages. When cells exit the mitotic cycle, distal appendages of the mother centriole are remodeled and transformed into the basal body. OFD1 is also involved in the recruitment of IFT88, a protein of the intraflagellar transport system. According with the requirement of both distal appendages and IFT88 for primary ciliogenesis, mutations of OFD1 inhibits primary cilia formation. This evidence demonstrates that centrosomal OFD1 is

required for primary ciliogenesis. In fact, OFD1 knockout induced a marked reduction of primary cilia (D'Angelo 2012; Ferrante 2009; Ferrante 2006).
cAMP signaling is involved in the regulation of primary cilia. Both catalytic and regulatory subunits of PKA have been identified within the ciliary compartment. Here, PKA activation tonically inhibits SHH pathway, inducing proteolysis of gli proteins and accumulation gli repressors (Wang 2000). The identification of the orphan receptor Gpr161 at the primary cilium provided a new link between cAMP/PKA and primary cilia. Thus, Gpr161 act as an AKAP that localizes PKA in the ciliary axoneme, controlling locally generated PKA signaling (Mukhopadhyay 2013).
I showed that cAMP, through the regulation of OFD1, induces cilia resorption. Thus, the stimulation of serum deprived cells with cAMP induces cilia disassembly that is reversed by the expression of a phospho-deficient mutant of OFD1. These findings are consistent with the role of cAMP in controlling cilium dynamics. Thus, in serum deprived cells, the stimulation with cAMP induces cilia resorption. This, at least in part, is due to the cAMP/PKA mediated proteolysis of Nima-related kinases NEK10. NEK10 has an essential role in cilia formation; cAMP stimulation induces NEK10 ubiquitylation and proteolysis mediated by the E3 ligases CHIP, inducing cilium disassembly (Porpora, 2018). However, cAMP can also promote ciliogenesis. In serum supplemented confluent cells, cAMP enhances the speed of anterograde flux, increasing cilium length (Besschetnova 2010). The apparently opposite roles of cAMP in cilium dynamics are related to different growth conditions that probably modify the sensitivity of the ciliary compartment to cAMP. The different growth conditions may, thus, shift the sensitivity of the system to cAMP and/or modulate the dissemination of cAMP signals to the ciliary compartment. In this context, nanobody-based optogenetic tools have revealed the spatial contribution of cAMP signalling in cilium biology and dynamics. Thus, high cAMP levels within the cilium increase the axonemal length, whereas accumulation of cAMP within the cell body by membrane GPCR activation reduced cilium length.

The phospho-deficient mutant of OFD1 (S735A) leads to generation of cilia with altered morphology and fragmentations along the axoneme. Defects in cilium morphology can alter the activation of SHH pathway. Thus, I found that the expression of OFD1 S735A drastically abolished the transcription of gli2 mRNA in SHH-stimulated cells. SHH signaling is strictly dependent on the IFT machinery, that localizes components of the pathway in the ciliary compartment. Accordingly, an altered structure of ciliary shape can determine an impairment of the pathway (Huangfu 2003).

Another interesting aspect of my study is the finding that a ciliopathy-related mutant OFD1 (E97G) was not degraded by cAMP stimulation. E97G is a mutation located in the LisH domain that causes the Oro Facial Digital syndrome (Macca 2009). The LisH domain is necessary for OFD1-mediated recruitment of IFT88; thus, mutations in this domain have a major impact on primary ciliogenesis (Singla 2010). The finding that E97G mutant of OFD1 is resistant to cAMP-mediated proteolysis, supports the hypothesis that cAMP-mediated removal of OFD1 is an important mechanism for cilium biology.

The ciliary phenotype I observed in cells expressing OFD1 mutations was confirmed also in Medaka fish, an animal model widely used to study processes involved in vertebrate development. Knock-down of TBC1D31 in Medaka fish alters the ciliogenesis and induces major developmental defects. Concomitant overexpression of OFD1 didn't rescue the phenotype induced by TBC1D31 knockdown, possibly because TBC1D31 depletion directly affects praja2/PKA/OFD1 molecular network at centrosome. Phosphorylation of OFD1 has a crucial role in development of Medaka fish. Thus, OFD1 S735A overexpression generates a dramatic phenotype, similar to that observed in the TBC1D31 knockdown fish. Co-expressing praja2 rm mutant and a phospho-mimetic OFD1 mutant (S735D) rescued the ciliogenic defects and the development of TBC1D31-knocked down Medaka fish embryos. This indicates that TBC1D31 is essential to assemble the praja2/OFD1/PKA complex in which OFD1 is phosphorylated by PKA and ubiquitylated and proteolyzed by praja2;

these events are necessary to the normal dynamic of primary cilia and also for the correct development.

6. Conclusion

Here I described the identification of a centrosomal transduction unit regulated by cAMP that is involved in primary ciliogenesis and development. TBC1D31 is a centrosomal protein that acts as a scaffold to assemble a multimeric complex constituted by the ciliary protein OFD1, the E3 ubiquitin ligase praja2 and PKA. In response to GPCRs stimulation, cAMP induces PKA-mediated phosphorylation of OFD1 that is coupled to its ubiquitylation and proteolysis by praja2 within the same complex. The cAMP mediated regulation of this complex is involved in the control of primary cilia dynamics. By controlling OFD1 levels, this regulatory circuitry significantly impacts on cilium biology and development, with important implications for genetic and proliferative disorders.

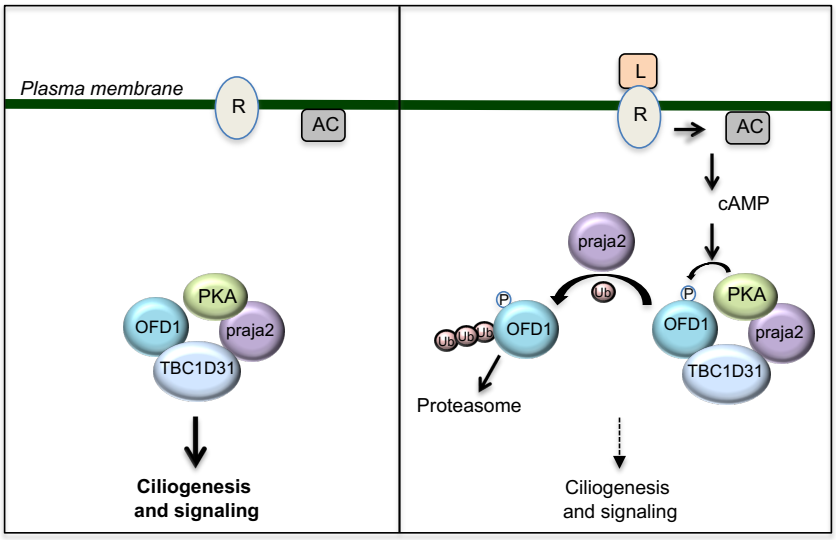

Figure 28. TBC1D31 assembled complex regulates ciliogenesis and signaling. GPCRs stimulation activates adenylate cyclase that raises cAMP levels, that in turn activates PKA. PKA phosphorylates OFD1 on the serine 735, promoting its ubiquitylation and proteolysis by praja2. The reduction of OFD1 levels impacts on primary ciliogenesis and signaling.

7. Acknowledgement

For contribution in my thesis project, I would thank prof. Ivan Conte and dr. Daniela Intartaglia for designing and performing experiments in Medaka fish.

I would also thank prof. Brunella Franco for kindly providing OFD1 plasmids and for helping with acquisition of superresolution confocal images.

8. List of publications

Senatore E, Chiuso F, Rinaldi L, Intartaglia D, Delle Donne R, Pedone E, Catalanotti B, Pirone L, Fiorillo F, Moraca F, Giamundo G, Scala G, Raffeiner A, Torres-Quesada O, Stefan E, Kwiatkowski M, van Pijkeren A, Morleo M, Franco B, Garbi C, Conte I, Feliciello A. The TBC1D31/praja2 complex controls primary ciliogenesis through PKA-directed OFD1 ubiquitylation. (2021) Embo J.

9. References

Alby C, Piquand K, Huber C, Megarbané A, Ichkou A, Legendre M, Pelluard F, Encha-Ravazi F, Abi-Tayeh G, Bessières B, El Chehadeh-Djebbar S, Laurent N, Faivre L, Sztriha L, Zombor M, Szabó H, Failler M, Garfa-Traore M, Bole C, Nitschké P, Nizon M, Elkhartoufi N, Clerget-Darpoux F, Munnich A, Lyonnet S, Vekemans M, Saunier S, Cormier-Daire V, Attié-Bitach T, Thomas S. 2015. Mutations in KIAA0586 Cause Lethal Ciliopathies Ranging from a Hydrolethalus Phenotype to Short-Rib Polydactyly Syndrome. Am J Hum Genet 97:311–318. doi:10.1016/j.ajhg.2015.06.003

Amerik AY, Hochstrasser M. 2004. Mechanism and function of deubiquitinating enzymes. Biochim Biophys Acta 1695:189–207. doi:10.1016/j.bbamcr.2004.10.003

Armstrong R, Wen W, Meinkoth J, Taylor S, Montminy M. 1995. A refractory phase in cyclic AMP-responsive transcription requires down regulation of protein kinase A. Mol Cell Biol 15:1826–1832. doi:10.1128/mcb.15.3.1826

Avellino R, Carrella S, Pirozzi M, Risolino M, Salierno FG, Franco P, Stoppelli P, Verde P, Banfi S, Conte I. 2013. miR-204 targeting of Ankrd13A controls both mesenchymal neural crest and lens cell migration. PLoS One 8:e61099. doi:10.1371/journal.pone.0061099

Avidor-Reiss T, Leroux MR. 2015. Shared and Distinct Mechanisms of Compartmentalized and Cytosolic Ciliogenesis. Curr Biol 25:R1143-1150. doi:10.1016/j.cub.2015.11.001

Bachmann VA, Mayrhofer JE, Ilouz R, Tschaikner P, Raffeiner P, Röck R, Courcelles M, Apelt F, Lu T-W, Baillie GS, Thibault P, Aanstad P, Stelzl U, Taylor SS, Stefan E. 2016. Gpr161 anchoring of PKA consolidates GPCR and cAMP signaling. Proc Natl Acad Sci U S A 113:7786–7791. doi:10.1073/pnas.1608061113

Badano JL, Mitsuma N, Beales PL, Katsanis N. 2006. The ciliopathies: an emerging class of human genetic disorders. Annu Rev Genomics Hum Genet

7:125–148. doi:10.1146/annurev.genom.7.080505.115610

Bangs F, Anderson KV. 2017. Primary Cilia and Mammalian Hedgehog Signaling. Cold Spring Harb Perspect Biol 9. doi:10.1101/cshperspect.a028175

Bard JAM, Goodall EA, Greene ER, Jonsson E, Dong KC, Martin A. 2018. Structure and Function of the 26S Proteasome. Annu Rev Biochem 87:697–724. doi:10.1146/annurev-biochem-062917-011931

Barr MM, Sternberg PW. 1999. A polycystic kidney-disease gene homologue required for male mating behaviour in C. elegans. Nature 401:386–389. doi:10.1038/43913

Barzi M, Berenguer J, Menendez A, Alvarez-Rodriguez R, Pons S. 2010. Sonic-hedgehog-mediated proliferation requires the localization of PKA to the cilium base. J Cell Sci 123:62–69. doi:10.1242/jcs.060020

Beck F, Unverdorben P, Bohn S, Schweitzer A, Pfeifer G, Sakata E, Nickell S, Plitzko JM, Villa E, Baumeister W, Forster F. 2012. Near-atomic resolution structural model of the yeast 26S proteasome. Proceedings of the National Academy of Sciences 109:14870–14875. doi:10.1073/pnas.1213333109

Berbari NF, Johnson AD, Lewis JS, Askwith CC, Mykytyn K. 2008. Identification of ciliary localization sequences within the third intracellular loop of G protein-coupled receptors. Mol Biol Cell 19:1540–1547. doi:10.1091/mbc.e07-09-0942

Besschetnova TY, Kolpakova-Hart E, Guan Y, Zhou J, Olsen BR, Shah JV. 2010. Identification of signaling pathways regulating primary cilium length and flow-mediated adaptation. Curr Biol 20:182–187. doi:10.1016/j.cub.2009.11.072

Blacque OE, Leroux MR. 2006. Bardet-Biedl syndrome: an emerging pathomechanism of intracellular transport. Cell Mol Life Sci 63:2145–2161. doi:10.1007/s00018-006-6180-x

Borodovsky A, Kessler BM, Casagrande R, Overkleeft HS, Wilkinson KD,

Ploegh HL. 2001. A novel active site-directed probe specific for deubiquitylating enzymes reveals proteasome association of USP14. EMBO J 20:5187–5196. doi:10.1093/emboj/20.18.5187

Burgers PP, Ma Y, Margarucci L, Mackey M, van der Heyden MAG, Ellisman M, Scholten A, Taylor SS, Heck AJR. 2012. A Small Novel A-Kinase Anchoring Protein (AKAP) That Localizes Specifically Protein Kinase A-Regulatory Subunit I (PKA-RI) to the Plasma Membrane. Journal of Biological Chemistry 287:43789–43797. doi:10.1074/jbc.M112.395970

Burton KA, Johnson BD, Hausken ZE, Westenbroek RE, Idzerda RL, Scheuer T, Scott JD, Catterall WA, McKnight GS. 1997. Type II regulatory subunits are not required for the anchoring-dependent modulation of Ca2+ channel activity by cAMP-dependent protein kinase. Proceedings of the National Academy of Sciences 94:11067–11072. doi:10.1073/pnas.94.20.11067

Callis J. 2014. The ubiquitylation machinery of the ubiquitin system. Arabidopsis Book 12:e0174. doi:10.1199/tab.0174

Carnegie GK. 2003. A-kinase anchoring proteins and neuronal signaling mechanisms. Genes & Development 17:1557–1568. doi:10.1101/gad.1095803

Carr DW, Stofko-Hahn RE, Fraser ID, Cone RD, Scott JD. 1992. Localization of the cAMP-dependent protein kinase to the postsynaptic densities by A-kinase anchoring proteins. Characterization of AKAP 79. J Biol Chem 267:16816–16823.

Chen Y, Yue S, Xie L, Pu X, Jin T, Cheng SY. 2011. Dual Phosphorylation of suppressor of fused (Sufu) by PKA and GSK3beta regulates its stability and localization in the primary cilium. J Biol Chem 286:13502–13511. doi:10.1074/jbc.M110.217604

Cole DG, Diener DR, Himelblau AL, Beech PL, Fuster JC, Rosenbaum JL. 1998. Chlamydomonas kinesin-II-dependent intraflagellar transport (IFT): IFTparticles contain proteins required for ciliary assembly in Caenorhabditis

elegans sensory neurons. J Cell Biol 141:993–1008. doi:10.1083/jcb.141.4.993

Collins GA, Goldberg AL. 2017. The Logic of the 26S Proteasome. Cell 169:792–806. doi:10.1016/j.cell.2017.04.023

Conte I, Carrella S, Avellino R, Karali M, Marco-Ferreres R, Bovolenta P, Banfi S. 2010. miR-204 is required for lens and retinal development via Meis2 targeting. Proceedings of the National Academy of Sciences 107:15491–15496. doi:10.1073/pnas.0914785107

Cooper DMF, Tabbasum VG. 2014. Adenylate cyclase-centred microdomains. Biochemical Journal 462:199–213. doi:10.1042/BJ20140560

Corbit KC, Shyer AE, Dowdle WE, Gaulden J, Singla V, Chen M-H, Chuang P-T, Reiter JF. 2008. Kif3a constrains beta-catenin-dependent Wnt signalling through dual ciliary and non-ciliary mechanisms. Nat Cell Biol 10:70–76. doi:10.1038/ncb1670

Craige B, Witman GB. 2014. Flipping a phosphate switch on kinesin-II to turn IFTaround. Dev Cell 30:492–493. doi:10.1016/j.devcel.2014.08.019

Cueva JG, Hsin J, Huang KC, Goodman MB. 2012. Posttranslational acetylation of α-tubulin constrains protofilament number in native microtubules. Curr Biol 22:1066–1074. doi:10.1016/j.cub.2012.05.012

Cygnar KD, Zhao H. 2009. Phosphodiesterase 1C is dispensable for rapid response termination of olfactory sensory neurons. Nat Neurosci 12:454–462. doi:10.1038/nn.2289

D'Angelo A, De Angelis A, Avallone B, Piscopo I, Tammaro R, Studer M, Franco B. 2012. Ofd1 controls dorso-ventral patterning and axoneme elongation during embryonic brain development. PLoS One 7:e52937. doi:10.1371/journal.pone.0052937

D'Angiolella V, Donato V, Vijayakumar S, Saraf A, Florens L, Washburn MP, Dynlacht B, Pagano M. 2010. SCF(Cyclin F) controls centrosome homeostasis and mitotic fidelity through CP110 degradation. Nature 466:138–142.

doi:10.1038/nature09140

Davis EE, Katsanis N. 2012. The ciliopathies: a transitional model into systems biology of human genetic disease. Curr Opin Genet Dev 22:290–303. doi:10.1016/j.gde.2012.04.006

de Conciliis L, Marchitiello A, Wapenaar MC, Borsani G, Giglio S, Mariani M, Consalez GG, Zuffardi O, Franco B, Ballabio A, Banfi S. 1998. Characterization of Cxorf5 (71-7A), a novel human cDNA mapping to Xp22 and encoding a protein containing coiled-coil alpha-helical domains. Genomics 51:243–250. doi:10.1006/geno.1998.5348

Dikic I. 2017. Proteasomal and Autophagic Degradation Systems. Annu Rev Biochem 86:193–224. doi:10.1146/annurev-biochem-061516-044908

Dodge KL, Khouangsathiene S, Kapiloff MS, Mouton R, Hill EV, Houslay MD, Langeberg LK, Scott JD. 2001. mAKAP assembles a protein kinase A/PDE4 phosphodiesterase cAMP signaling module. EMBO J 20:1921–1930. doi:10.1093/emboj/20.8.1921

Eccles RL, Czajkowski MT, Barth C, Müller PM, McShane E, Grunwald S, Beaudette P, Mecklenburg N, Volkmer R, Zühlke K, Dittmar G, Selbach M, Hammes A, Daumke O, Klussmann E, Urbé S, Rocks O. 2016. Bimodal antagonism of PKA signalling by ARHGAP36. Nat Commun 7:12963. doi:10.1038/ncomms12963

Emes RD, Ponting CP. 2001. A new sequence motif linking lissencephaly, Treacher Collins and oral-facial-digital type 1 syndromes, microtubule dynamics and cell migration. Hum Mol Genet 10:2813–2820. doi:10.1093/hmg/10.24.2813

Feather SA, Woolf AS, Donnai D, Malcolm S, Winter RM. 1997. The oral-facial-digital syndrome type 1 (OFD1), a cause of polycystic kidney disease and associated malformations, maps to Xp22.2-Xp22.3. Hum Mol Genet 6:1163–1167. doi:10.1093/hmg/6.7.1163

Feliciello A, Gottesman ME, Avvedimento EV. 2001. The biological functions of A-kinase anchor proteins. J Mol Biol 308:99–114. doi:10.1006/jmbi.2001.4585

Ferrante MI, Giorgio G, Feather SA, Bulfone A, Wright V, Ghiani M, Selicorni A, Gammaro L, Scolari F, Woolf AS, Sylvie O, Bernard L, Malcolm S, Winter R, Ballabio A, Franco B. 2001. Identification of the gene for oral-facial-digital type I syndrome. Am J Hum Genet 68:569–576. doi:10.1086/318802

Ferrante MI, Romio L, Castro S, Collins JE, Goulding DA, Stemple DL, Woolf AS, Wilson SW. 2009. Convergent extension movements and ciliary function are mediated by ofd1, a zebrafish orthologue of the human oral-facial-digital type 1 syndrome gene. Hum Mol Genet 18:289–303. doi:10.1093/hmg/ddn356

Ferrante MI, Zullo A, Barra A, Bimonte S, Messaddeq N, Studer M, Dollé P, Franco B. 2006. Oral-facial-digital type I protein is required for primary cilia formation and left-right axis specification. Nat Genet 38:112–117. doi:10.1038/ng1684

Finley D, Chen X, Walters KJ. 2016. Gates, Channels, and Switches: Elements of the Proteasome Machine. Trends Biochem Sci 41:77–93. doi:10.1016/j.tibs.2015.10.009

Francis SH, Blount MA, Corbin JD. 2011. Mammalian Cyclic Nucleotide Phosphodiesterases: Molecular Mechanisms and Physiological Functions. Physiological Reviews 91:651–690. doi:10.1152/physrev.00030.2010

Franco B, Thauvin-Robinet C. 2016. Update on oral-facial-digital syndromes (OFDS). Cilia 5:12. doi:10.1186/s13630-016-0034-4

Fraser ID, Scott JD. 1999. Modulation of ion channels: a “current” view of AKAPs. Neuron 23:423–426. doi:10.1016/s0896-6273(00)80795-3

Freemont PS. 1993. The RING finger. A novel protein sequence motif related to the zinc finger. Ann N Y Acad Sci 684:174–192. doi:10.1111/j.1749-

6632.1993.tb32280.x

Fu H, Sadis S, Rubin DM, Glickman M, van Nocker S, Finley D, Vierstra RD. 1998. Multiubiquitin Chain Binding and Protein Degradation Are Mediated by Distinct Domains within the 26 S Proteasome Subunit Mcb1. Journal of Biological Chemistry 273:1970–1981. doi:10.1074/jbc.273.4.1970

Giorgio G, Alfieri M, Prattichizzo C, Zullo A, Cairo S, Franco B. 2007. Functional characterization of the OFD1 protein reveals a nuclear localization and physical interaction with subunits of a chromatin remodeling complex. Mol Biol Cell 18:4397–4404. doi:10.1091/mbc.e07-03-0198

Goetz SC, Anderson KV. 2010. The primary cilium: a signalling centre during vertebrate development. Nat Rev Genet 11:331–344. doi:10.1038/nrg2774

Gupta GD, Coyaud É, Gonçalves J, Mojarad BA, Liu Y, Wu Q, Gheiratmand L, Comartin D, Tkach JM, Cheung SWT, Bashkurov M, Hasegan M, Knight JD, Lin Z-Y, Schueler M, Hildebrandt F, Moffat J, Gingras A-C, Raught B, Pelletier L. 2015. A Dynamic Protein Interaction Landscape of the Human Centrosome-Cilium Interface. Cell 163:1484–1499. doi:10.1016/j.cell.2015.10.065

Haglund K, Dikic I. 2005. Ubiquitylation and cell signaling. EMBO J 24:3353–3359. doi:10.1038/sj.emboj.7600808

Hansen JN, Kaiser F, Klausen C, Stüven B, Chong R, Bönigk W, Mick DU, Möglich A, Jurisch-Yaksi N, Schmidt FI, Wachten D. 2020. Nanobody-directed targeting of optogenetic tools to study signaling in the primary cilium. Elife 9. doi:10.7554/eLife.57907

Hepler JR, Gilman AG. 1992. G proteins. Trends in Biochemical Sciences 17:383–387. doi:10.1016/0968-0004(92)90005-T

Hilgendorf KI, Johnson CT, Jackson PK. 2016. The primary cilium as a cellular receiver: organizing ciliary GPCR signaling. Curr Opin Cell Biol 39:84–92. doi:10.1016/j.ceb.2016.02.008

Hossain D, Tsang WY. 2019. The role ofubiquitylation in the regulation of primary cilia assembly and disassembly. Semin Cell Dev Biol 93:145–152. doi:10.1016/j.semcdb.2018.09.005

Huangfu D, Liu A, Rakeman AS, Murcia NS, Niswander L, Anderson KV. 2003. Hedgehog signalling in the mouse requires intraflagellar transport proteins. Nature 426:83–87. doi:10.1038/nature02061

Humbert MC, Weihbrecht K, Searby CC, Li Y, Pope RM, Sheffield VC, Seo S. 2012. ARL13B, PDE6D, and CEP164 form a functional network for INPP5E ciliary targeting. Proceedings of the National Academy of Sciences 109:19691–19696. doi:10.1073/pnas.1210916109

Husnjak K, Dikic I. 2012. Ubiquitin-binding proteins: decoders of ubiquitin-mediated cellular functions. Annu Rev Biochem 81:291–322. doi:10.1146/annurev-biochem-051810-094654

Ikeda F, Dikic I. 2008. Atypical ubiquitin chains: new molecular signals. "Protein Modifications: Beyond the Usual Suspects" review series. EMBO Rep 9:536–542. doi:10.1038/embor.2008.93

Ishikawa H, Marshall WF. 2011. Ciliogenesis: building the cell's antenna. Nat Rev Mol Cell Biol 12:222–234. doi:10.1038/nrm3085

Iyengar R. 1993. Molecular and functional diversity of mammalian G_s-stimulated adenylyl cyclases. FASEB j 7:768–775. doi:10.1096/fasebj.7.9.8330684

Jin S-LC, Bushnik T, Lan L, Conti M. 1998. Subcellular Localization of Rolipram-sensitive, cAMP-specific Phosphodiesterases. Journal of Biological Chemistry 273:19672–19678. doi:10.1074/jbc.273.31.19672

Johnson KA, Rosenbaum JL. 1992. Polarity of flagellar assembly in Chlamydomonas. J Cell Biol 119:1605–1611. doi:10.1083/jcb.119.6.1605

Kasahara K, Kawakami Y, Kiyono T, Yonemura S, Kawamura Y, Era S, Matsuzaki F, Goshima N, Inagaki M. 2014. Ubiquitin-proteasome system

controls ciliogenesis at the initial step of axoneme extension. Nat Commun 5:5081. doi:10.1038/ncomms6081

Kaupp UB. 2010. Olfactory signalling in vertebrates and insects: differences and commonalities. Nat Rev Neurosci 11:188–200. doi:10.1038/nrn2789

Kisselev AF, Akopian TN, Castillo V, Goldberg AL. 1999. Proteasome active sites allosterically regulate each other, suggesting a cyclical bite-chew mechanism for protein breakdown. Mol Cell 4:395–402. doi:10.1016/s1097-2765(00)80341-x

Knighton D, Zheng J, Ten Eyck L, Ashford V, Xuong N, Taylor S, Sowadski J. 1991. Crystal structure of the catalytic subunit of cyclic adenosine monophosphate-dependent protein kinase. Science 253:407–414. doi:10.1126/science.1862342

Kozminski KG, Johnson KA, Forscher P, Rosenbaum JL. 1993. A motility in the eukaryotic flagellum unrelated to flagellar beating. Proc Natl Acad Sci U S A 90:5519–5523. doi:10.1073/pnas.90.12.5519

L'Hernault SW, Rosenbaum JL. 1983. Chlamydomonas alpha-tubulin is posttranslationally modified in the flagella during flagellar assembly. J Cell Biol 97:258–263. doi:10.1083/jcb.97.1.258

Li J, D'Angiolella V, Seeley ES, Kim S, Kobayashi T, Fu W, Campos EI, Pagano M, Dynlacht BD. 2013. USP33 regulates centrosome biogenesis via deubiquitination of the centriolar protein CP110. Nature 495:255–259. doi:10.1038/nature11941

Lignitto L, Arcella A, Sepe M, Rinaldi L, Delle Donne R, Gallo A, Stefan E, Bachmann VA, Oliva MA, Tiziana Storlazzi C, L'Abbate A, Brunetti A, Gargiulo S, Gramanzini M, Insabato L, Garbi C, Gottesman ME, Feliciello A. 2013. Proteolysis of MOB1 by the ubiquitin ligase praja2 attenuates Hippo signalling and supports glioblastoma growth. Nat Commun 4:1822. doi:10.1038/ncomms2791

Lignitto L, Carlucci A, Sepe M, Stefan E, Cuomo O, Nisticò R, Scorziello A, Savoia C, Garbi C, Annunziato L, Feliciello A. 2011. Control of PKA stability and signalling by the RING ligase praja2. Nat Cell Biol 13:412–422. doi:10.1038/ncb2209

Lilienbaum A. 2013. Relationship between the proteasomal system and autophagy. Int J Biochem Mol Biol 4:1–26.

Liu C-W, Jacobson AD. 2013. Functions of the 19S complex in proteasomal degradation. Trends Biochem Sci 38:103–110. doi:10.1016/j.tibs.2012.11.009

Lopes CAM, Prosser SL, Romio L, Hirst RA, O'Callaghan C, Woolf AS, Fry AM. 2011. Centriolar satellites are assembly points for proteins implicated in human ciliopathies, including oral-facial-digital syndrome 1. J Cell Sci 124:600–612. doi:10.1242/jcs.077156

Macca M, Franco B. 2009. The molecular basis of oral-facial-digital syndrome, type 1. Am J Med Genet C Semin Med Genet 151C:318–325. doi:10.1002/ajmg.c.30224

McConnachie G, Langeberg LK, Scott JD. 2006. AKAP signaling complexes: getting to the heart of the matter. Trends Mol Med 12:317–323. doi:10.1016/j.molmed.2006.05.008

McMahon AP, Ingham PW, Tabin CJ. 2003. Developmental roles and clinical significance of hedgehog signaling. Curr Top Dev Biol 53:1–114. doi:10.1016/s0070-2153(03)53002-2

Metzger MB, Pruneda JN, Klevit RE, Weissman AM. 2014. RING-type E3 ligases: Master manipulators of E2 ubiquitin-conjugating enzymes and ubiquitination. Biochimica et Biophysica Acta (BBA) - Molecular Cell Research 1843:47–60. doi:10.1016/j.bbamcr.2013.05.026

Michel JJC, Scott JD. 2002. AKAP mediated signal transduction. Annu Rev Pharmacol Toxicol 42:235–257. doi:10.1146/annurev.pharmtox.42.083101.135801

Mick DU, Rodrigues RB, Leib RD, Adams CM, Chien AS, Gygi SP, Nachury MV. 2015. Proteomics of Primary Cilia by Proximity Labeling. Dev Cell 35:497–512. doi:10.1016/j.devcel.2015.10.015

Mitchison HM, Valente EM. 2017. Motile and non-motile cilia in human pathology: from function to phenotypes. J Pathol 241:294–309. doi:10.1002/path.4843

Miyamoto T, Hosoba K, Ochiai H, Royba E, Izumi H, Sakuma T, Yamamoto T, Dynlacht BD, Matsuura S. 2015. The Microtubule-Depolymerizing Activity of a Mitotic Kinesin Protein KIF2A Drives Primary Cilia Disassembly Coupled with Cell Proliferation. Cell Rep 10:664–673. doi:10.1016/j.celrep.2015.01.003

Moore BS, Stepanchick AN, Tewson PH, Hartle CM, Zhang J, Quinn AM, Hughes TE, Mirshahi T. 2016. Cilia have high cAMP levels that are inhibited by Sonic Hedgehog-regulated calcium dynamics. Proc Natl Acad Sci USA 113:13069–13074. doi:10.1073/pnas.1602393113

Mukhopadhyay S, Wen X, Ratti N, Loktev A, Rangell L, Scales SJ, Jackson PK. 2013. The Ciliary G-Protein-Coupled Receptor Gpr161 Negatively Regulates the Sonic Hedgehog Pathway via cAMP Signaling. Cell 152:210–223. doi:10.1016/j.cell.2012.12.026

Mykytyn K, Askwith C. 2017. G-Protein-Coupled Receptor Signaling in Cilia. Cold Spring Harb Perspect Biol 9. doi:10.1101/cshperspect.a028183

Newlon MG. 2001. A novel mechanism of PKA anchoring revealed by solution structures of anchoring complexes. The EMBO Journal 20:1651–1662. doi:10.1093/emboj/20.7.1651

Ogden SK, Fei DL, Schilling NS, Ahmed YF, Hwa J, Robbins DJ. 2008. G protein Galphai functions immediately downstream of Smoothened in Hedgehog signalling. Nature 456:967–970. doi:10.1038/nature07459

Pampliega O, Orhon I, Patel B, Sridhar S, Díaz-Carretero A, Beau I, Codogno

P, Satir BH, Satir P, Cuervo AM. 2013. Functional interaction between autophagy and ciliogenesis. Nature 502:194–200. doi:10.1038/nature12639

Parisi MA, Bennett CL, Eckert ML, Dobyns WB, Gleeson JG, Shaw DWW, McDonald R, Eddy A, Chance PF, Glass IA. 2004. The NPHP1 gene deletion associated with juvenile nephronophthisis is present in a subset of individuals with Joubert syndrome. Am J Hum Genet 75:82–91. doi:10.1086/421846

Pazour GJ, Wilkerson CG, Witman GB. 1998. A dynein light chain is essential for the retrograde particle movement of intraflagellar transport (IFT). J Cell Biol 141:979–992. doi:10.1083/jcb.141.4.979

Pennekamp P, Karcher C, Fischer A, Schweickert A, Skryabin B, Horst J, Blum M, Dworniczak B. 2002. The ion channel polycystin-2 is required for left-right axis determination in mice. Curr Biol 12:938–943. doi:10.1016/s0960-9822(02)00869-2

Piel M, Meyer P, Khodjakov A, Rieder CL, Bornens M. 2000. The respective contributions of the mother and daughter centrioles to centrosome activity and behavior in vertebrate cells. J Cell Biol 149:317–330. doi:10.1083/jcb.149.2.317

Plotnikova OV, Nikonova AS, Loskutov YV, Kozyulina PY, Pugacheva EN, Golemis EA. 2012. Calmodulin activation of Aurora-A kinase (AURKA) is required during ciliary disassembly and in mitosis. Mol Biol Cell 23:2658–2670. doi:10.1091/mbc.E11-12-1056

Plotnikova OV, Pugacheva EN, Golemis EA. 2009. Primary cilia and the cell cycle. Methods Cell Biol 94:137–160. doi:10.1016/S0091-679X(08)94007-3

Pohl C, Dikic I. 2019. Cellular quality control by the ubiquitin-proteasome system and autophagy. Science 366:818–822. doi:10.1126/science.aax3769

Porpora M, Sauchella S, Rinaldi L, Delle Donne R, Sepe M, Torres-Quesada O, Intartaglia D, Garbi C, Insabato L, Santoriello M, Bachmann VA, Synofzik M, Lindner HH, Conte I, Stefan E, Feliciello A. 2018. Counterregulation of cAMP-directed kinase activities controls ciliogenesis. Nat Commun 9:1224. doi:10.1038/s41467-018-03643-9

Prattichizzo C, Macca M, Novelli V, Giorgio G, Barra A, Franco B, Oral-Facial-Digital Type I (OFDI) Collaborative Group. 2008. Mutational spectrum of the oral-facial-digital type I syndrome: a study on a large collection of patients. Hum Mutat 29:1237–1246. doi:10.1002/humu.20792

Pugacheva EN, Jablonski SA, Hartman TR, Henske EP, Golemis EA. 2007. HEF1-dependent Aurora A activation induces disassembly of the primary cilium. Cell 129:1351–1363. doi:10.1016/j.cell.2007.04.035

Rajagopal S, Shenoy SK. 2018. GPCR desensitization: Acute and prolonged phases. Cellular Signalling 41:9–16. doi:10.1016/j.cellsig.2017.01.024

Reiter E, Lefkowitz RJ. 2006. GRKs and β-arrestins: roles in receptor silencing, trafficking and signaling. Trends in Endocrinology & Metabolism 17:159–165. doi:10.1016/j.tem.2006.03.008

Reiter JF, Leroux MR. 2017. Genes and molecular pathways underpinning ciliopathies. Nat Rev Mol Cell Biol 18:533–547. doi:10.1038/nrm.2017.60

Rinaldi L, Delle Donne R, Catalanotti B, Torres-Quesada O, Enzler F, Moraca F, Nisticò R, Chiuso F, Piccinin S, Bachmann V, Lindner HH, Garbi C, Scorziello A, Russo NA, Synofzik M, Stelzl U, Annunziato L, Stefan E, Feliciello A. 2019. Feedback inhibition of cAMP effector signaling by a chaperone-assisted ubiquitin system. Nat Commun 10:2572. doi:10.1038/s41467-019-10037-y

Rinaldi L, Delle Donne R, Sepe M, Porpora M, Garbi C, Chiuso F, Gallo A, Parisi S, Russo L, Bachmann V, Huber RG, Stefan E, Russo T, Feliciello A. 2016. praja2 regulates KSR1 stability and mitogenic signaling. Cell Death Dis 7:e2230. doi:10.1038/cddis.2016.109

Rinaldi L, Sepe M, Donne RD, Feliciello A. 2015. A dynamic interface between ubiquitylation and cAMP signaling. Front Pharmacol 6:177. doi:10.3389/fphar.2015.00177

Robbins DJ, Fei DL, Riobo NA. 2012. The Hedgehog signal transduction network. Sci Signal 5:re6. doi:10.1126/scisignal.2002906

Rohatgi R, Milenkovic L, Scott MP. 2007. Patched1 regulates hedgehog signaling at the primary cilium. Science 317:372–376. doi:10.1126/science.1139740

Romio L, Fry AM, Winyard PJD, Malcolm S, Woolf AS, Feather SA. 2004. OFD1 is a centrosomal/basal body protein expressed during mesenchymal-epithelial transition in human nephrogenesis. J Am Soc Nephrol 15:2556–2568. doi:10.1097/01.ASN.0000140220.46477.5C

Romio L, Wright V, Price K, Winyard PJD, Donnai D, Porteous ME, Franco B, Giorgio G, Malcolm S, Woolf AS, Feather SA. 2003. OFD1, the gene mutated in oral-facial-digital syndrome type 1, is expressed in the metanephros and in human embryonic renal mesenchymal cells. J Am Soc Nephrol 14:680–689. doi:10.1097/01.asn.0000054497.48394.d2

Rosenbaum DM, Rasmussen SGF, Kobilka BK. 2009. The structure and function of G-protein-coupled receptors. Nature 459:356–363. doi:10.1038/nature08144

Ruiz i Altaba A, Sánchez P, Dahmane N. 2002.gliand hedgehog in cancer: tumours, embryos and stem cells. Nat Rev Cancer 2:361–372. doi:10.1038/nrc796

Saha T, Vardhini D, Tang Y, Katuri V, Jogunoori W, Volpe EA, Haines D, Sidawy A, Zhou X, Gallicano I, Schlegel R, Mishra B, Mishra L. 2006. RING finger-dependentubiquitylation by PRAJA is dependent on TGF-beta and potentially defines the functional status of the tumor suppressor ELF. Oncogene 25:693–705. doi:10.1038/sj.onc.1209123

Sánchez I, Dynlacht BD. 2016. Cilium assembly and disassembly. Nat Cell Biol 18:711–717. doi:10.1038/ncb3370

Satir P, Christensen ST. 2007. Overview of structure and function of mammalian cilia. Annu Rev Physiol 69:377–400. doi:10.1146/annurev.physiol.69.040705.141236

Satir P, Pedersen LB, Christensen ST. 2010. The primary cilium at a glance. J Cell Sci 123:499–503. doi:10.1242/jcs.050377

Schmidt KN, Kuhns S, Neuner A, Hub B, Zentgraf H, Pereira G. 2012. Cep164 mediates vesicular docking to the mother centriole during early steps of ciliogenesis. J Cell Biol 199:1083–1101. doi:10.1083/jcb.201202126

Sepe M, Lignitto L, Porpora M, Delle Donne R, Rinaldi L, Belgianni G, Colucci G, Cuomo O, Viggiano D, Scorziello A, Garbi C, Annunziato L, Feliciello A. 2014. Proteolytic control of neurite outgrowth inhibitor NOGO-A by the cAMP/PKA pathway. Proc Natl Acad Sci U S A 111:15729–15734. doi:10.1073/pnas.1410274111

Signor D, Wedaman KP, Orozco JT, Dwyer ND, Bargmann CI, Rose LS, Scholey JM. 1999. Role of a class DHC1b dynein in retrograde transport of IFTmotors and IFTraft particles along cilia, but not dendrites, in chemosensory neurons of living Caenorhabditis elegans. J Cell Biol 147:519–530. doi:10.1083/jcb.147.3.519

Singh J, Wen X, Scales SJ. 2015. The Orphan G Protein-coupled Receptor Gpr175 (Tpra40) Enhances Hedgehog Signaling by Modulating cAMP Levels. J Biol Chem 290:29663–29675. doi:10.1074/jbc.M115.665810

Singla V, Romaguera-Ros M, Garcia-Verdugo JM, Reiter JF. 2010. Ofd1, a human disease gene, regulates the length and distal structure of centrioles. Dev Cell 18:410–424. doi:10.1016/j.devcel.2009.12.022

Skalhegg B S. 2000. Specificity in the cAMP/PKA signaling pathway. differential expression, regulation, and subcellular localization of subunits of PKA. Front Biosci 5:d678. doi:10.2741/Skalhegg

Smit JJ, Sixma TK. 2014. RBR E3-ligases at work. EMBO Rep 15:142–154. doi:10.1002/embr.201338166

Song Y, Lee S, Kim J-R, Jho E-H. 2018. Pja2 Inhibits Wnt/β-catenin Signaling by Reducing the Level of TCF/LEF1. Int J Stem Cells 11:242–247. doi:10.15283/ijsc18032

Sorokin SP. 1968. Centriole formation and ciliogenesis. Aspen Emphysema Conf 11:213–216.

Spassky N, Meunier A. 2017. The development and functions of multiciliated epithelia. Nat Rev Mol Cell Biol 18:423–436. doi:10.1038/nrm.2017.21

Stone M, Hartmann-Petersen R, Seeger M, Bech-Otschir D, Wallace M, Gordon C. 2004. Uch2/Uch37 is the major deubiquitinating enzyme associated with the 26S proteasome in fission yeast. J Mol Biol 344:697–706. doi:10.1016/j.jmb.2004.09.057

Sutherland EW, Rall TW. 1958. Fractionation and characterization of a cyclic adenine ribonucleotide formed by tissue particles. Journal of Biological Chemistry 232:1077–1091. doi:10.1016/S0021-9258(19)77423-7

Tang Z, Lin MG, Stowe TR, Chen S, Zhu M, Stearns T, Franco B, Zhong Q. 2013. Autophagy promotes primary ciliogenesis by removing OFD1 from centriolar satellites. Nature 502:254–257. doi:10.1038/nature12606

Taskén K, Aandahl EM. 2004. Localized Effects of cAMP Mediated by Distinct Routes of Protein Kinase A. Physiological Reviews 84:137–167. doi:10.1152/physrev.00021.2003

Taskén KA, Collas P, Kemmner WA, Witczak O, Conti M, Taskén K. 2001. Phosphodiesterase 4D and protein kinase a type II constitute a signaling unit in the centrosomal area. J Biol Chem 276:21999–22002. doi:10.1074/jbc.C000911200

Taylor SS, Buechler JA, Yonemoto W. 1990. cAMP-Dependent Protein Kinase: Framework for a Diverse Family of Regulatory Enzymes. Annu Rev Biochem 59:971–1005. doi:10.1146/annurev.bi.59.070190.004543

Taylor SS, Kim C, Vigil D, Haste NM, Yang J, Wu J, Anand GS. 2005. Dynamics of signaling by PKA. Biochimica et Biophysica Acta (BBA) - Proteins and Proteomics 1754:25–37. doi:10.1016/j.bbapap.2005.08.024

Taylor SS, Knighton DR, Zheng J, Sowadski JM, Gibbs CS, Zoller MJ. 1993. A template for the protein kinase family. Trends in Biochemical Sciences 18:84–89. doi:10.1016/0968-0004(93)80001-R

Taylor SS, Knighton DR, Zheng J, Ten Eyck LF, Sowadski JM. 1992. Structural Framework for the Protein Kinase Family. Annu Rev Cell Biol 8:429–462. doi:10.1146/annurev.cb.08.110192.002241

Tempé D, Casas M, Karaz S, Blanchet-Tournier M-F, Concordet J-P. 2006. Multisite protein kinase A and glycogen synthase kinase 3beta phosphorylation leads togli3ubiquitination by SCFbetaTrCP. Mol Cell Biol 26:4316–4326. doi:10.1128/MCB.02183-05

Thauvin-Robinet C, Franco B, Saugier-Veber P, Aral B, Gigot N, Donzel A, Van Maldergem L, Bieth E, Layet V, Mathieu M, Teebi A, Lespinasse J, Callier P, Mugneret F, Masurel-Paulet A, Gautier E, Huet F, Teyssier J-R, Tosi M, Frébourg T, Faivre L. 2009. Genomic deletions of OFD1 account for 23% of oral-facial-digital type 1 syndrome after negative DNA sequencing. Hum Mutat 30:E320-329. doi:10.1002/humu.20888

Theurkauf WE, Vallee RB. 1982. Molecular characterization of the cAMP-dependent protein kinase bound to microtubule-associated protein 2. J Biol Chem 257:3284–3290.

Torres VE, Harris PC, Pirson Y. 2007. Autosomal dominant polycystic kidney disease. Lancet 369:1287–1301. doi:10.1016/S0140-6736(07)60601-1

Torres-Quesada O, Mayrhofer JE, Stefan E. 2017. The many faces of compartmentalized PKA signalosomes. Cellular Signalling 37:1–11. doi:10.1016/j.cellsig.2017.05.012

Tuson M, He M, Anderson KV. 2011. Protein kinase A acts at the basal body of the primary cilium to preventgli2activation and ventralization of the mouse neural tube. Development 138:4921–4930. doi:10.1242/dev.070805

Wahrman J, Berant M, Jacobs J, Aviad I, Ben-Hur N. 1966. The oral-facial-digital syndrome: a male-lethal condition in a boy with 47/xxy chromosomes. Pediatrics 37:812–821.

Wang B, Fallon JF, Beachy PA. 2000. Hedgehog-regulated processing of Gli3 produces an anterior/posterior repressor gradient in the developing vertebrate limb. Cell 100:423–434. doi:10.1016/s0092-8674(00)80678-9

Webb S, Mukhopadhyay AG, Roberts AJ. 2020. Intraflagellar transport trains and motors: Insights from structure. Semin Cell Dev Biol 107:82–90. doi:10.1016/j.semcdb.2020.05.021

Wei Q, Zhang Y, Li Y, Zhang Q, Ling K, Hu J. 2012. The BBSome controls IFTassembly and turnaround in cilia. Nat Cell Biol 14:950–957. doi:10.1038/ncb2560

Weissman AM. 2001. Themes and variations on ubiquitylation. Nat Rev Mol Cell Biol 2:169–178. doi:10.1038/35056563

Wiegering A, Rüther U, Gerhardt C. 2019. The Role of Primary Cilia in the Crosstalk between the Ubiquitin–Proteasome System and Autophagy. Cells 8. doi:10.3390/cells8030241

Wilkinson KD. 2009. DUBs at a glance. J Cell Sci 122:2325–2329. doi:10.1242/jcs.041046

Winey M, O'Toole E. 2014. Centriole structure. Philos Trans R Soc Lond B Biol Sci 369. doi:10.1098/rstb.2013.0457

Wingfield JL, Mengoni I, Bomberger H, Jiang Y-Y, Walsh JD, Brown JM, Picariello T, Cochran DA, Zhu B, Pan J, Eggenschwiler J, Gaertig J, Witman GB, Kner P, Lechtreck K. 2017. IFTtrains in different stages of assembly queue at the ciliary base for consecutive release into the cilium. Elife 6. doi:10.7554/eLife.26609

Yu P, Chen Y, Tagle DA, Cai T. 2002. PJA1, Encoding a RING-H2 Finger Ubiquitin Ligase, Is a Novel Human X Chromosome Gene Abundantly Expressed in Brain. Genomics 79:869–874. doi:10.1006/geno.2002.6770

Zhao Z, Zhu L, Xing Y, Zhang Z. 2021. Praja2 suppresses the growth of gastric cancer by ubiquitylation of KSR1 and inhibiting MEK-ERK signal pathways. Aging (Albany NY) 13:3886–3897. doi:10.18632/aging.202356

Zhong J, Wang H, Chen W, Sun Z, Chen J, Xu Y, Weng M, Shi Q, Ma D, Miao C. 2017. Ubiquitylation of MFHAS1 by the ubiquitin ligase praja2 promotes M1 macrophage polarization by activating JNK and p38 pathways. Cell Death Dis 8:e2763–e2763. doi:10.1038/cddis.2017.102